

1995

A new stationary phase for reverse-phase high performance liquid chromatography

Ruby W. Tam
San Jose State University

Follow this and additional works at: https://scholarworks.sjsu.edu/etd_theses

Recommended Citation

Tam, Ruby W, "A new stationary phase for reverse-phase high performance liquid chromatography" (1995). *Master's Theses*. 1102.
DOI: <https://doi.org/10.31979/etd.rha9-vn65>
https://scholarworks.sjsu.edu/etd_theses/1102

This Thesis is brought to you for free and open access by the Master's Theses and Graduate Research at SJSU ScholarWorks. It has been accepted for inclusion in Master's Theses by an authorized administrator of SJSU ScholarWorks. For more information, please contact scholarworks@sjsu.edu.

INFORMATION TO USERS

This manuscript has been reproduced from the microfilm master. UMI films the text directly from the original or copy submitted. Thus, some thesis and dissertation copies are in typewriter face, while others may be from any type of computer printer.

The quality of this reproduction is dependent upon the quality of the copy submitted. Broken or indistinct print, colored or poor quality illustrations and photographs, print bleedthrough, substandard margins, and improper alignment can adversely affect reproduction.

In the unlikely event that the author did not send UMI a complete manuscript and there are missing pages, these will be noted. Also, if unauthorized copyright material had to be removed, a note will indicate the deletion.

Oversize materials (e.g., maps, drawings, charts) are reproduced by sectioning the original, beginning at the upper left-hand corner and continuing from left to right in equal sections with small overlaps. Each original is also photographed in one exposure and is included in reduced form at the back of the book.

Photographs included in the original manuscript have been reproduced xerographically in this copy. Higher quality 6" x 9" black and white photographic prints are available for any photographs or illustrations appearing in this copy for an additional charge. Contact UMI directly to order.

UMI

A Bell & Howell Information Company
300 North Zeeb Road, Ann Arbor, MI 48106-1346 USA
313/761-4700 800/521-0600

A NEW STATIONARY PHASE FOR REVERSE-PHASE HIGH PERFORMANCE
LIQUID CHROMATOGRAPHY

A Thesis

Presented to

The Faculty of the Department Of Chemistry

San Jose State University

In Partial Fulfillment

of the Requirement for the Degree

Master of Science

by

Ruby W. Tam

August, 1995

UMI Number: 1375726

UMI Microform 1375726

Copyright 1995, by UMI Company. All rights reserved.

**This microform edition is protected against unauthorized
copying under Title 17, United States Code.**

UMI

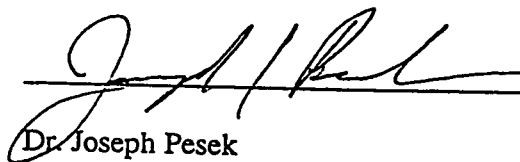
**300 North Zeeb Road
Ann Arbor, MI 48103**

© 1995

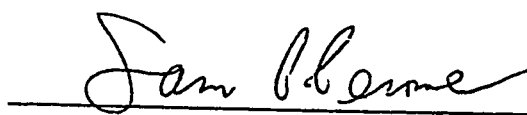
Ruby W. Tam

ALL RIGHTS RESERVED

APPROVED FOR THE DEPARTMENT OF CHEMISTRY



Dr. Joseph Pesek

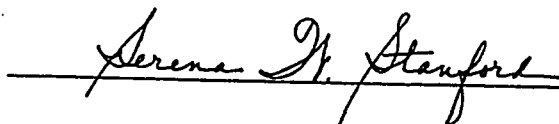


Dr. Sam Perone



Dr. Pam Stacks

APPROVED FOR THE UNIVERSITY



ABSTRACT

A NEW STATIONARY PHASE FOR REVERSE-PHASE HIGH PERFORMANCE LIQUID CHROMATOGRAPHY

by Ruby W. Tam

The optimized hydrosilation-reaction conditions successfully bonded 1.66 μmole of 4-methoxyphenol-4-allyloxybenzoate (MPAB) on each square-meter of silica surface. The MPAB-silica hydrosilation was catalyzed by chloroplatinic acid hexahydrate in isopentanol. Chromatographic studies showed that the resolution and the isomeric selectivity of a polyaromatic-hydrocarbon mixture on the MPAB stationary phase increased with surface coverage. The molecular alignment of the 1.66- $\mu\text{mole}/\text{m}^2$ -MPAB stationary phase resembled that of the oligomeric-polymeric C18 stationary phase. The retention mechanisms of MPAB and C18 phases are comparable.

Acknowledgments

Support from many people contributed to the success of this research. First, Dr. J. Pesek, Dr. S. Perone, Dr. P. Stacks and Dr. E. Williamsen reviewed my manuscript. Dr. J. Pesek and Dr. M. Matyska performed the ^{13}C and ^{29}Si nuclear magnetic resonance analyses for my silica samples. Dr. E. Williamsen analyzed the native silica and the silica hydride samples by the DRIFT technique, and packed the bonded silicas into stainless-steel columns. Dr. S. Perone and Dr. P. Stacks sat on my thesis committee. In addition, Dr. J. Sandoval offered me considerable encouragement and research insights. Lastly, Ray Berryesa and Richard Mercurio repaired the broken equipment in the least amount of time, so that I could finish this project in a timely manner.

Table of Contents

| | |
|---|-----------|
| CHAPTER I - INTRODUCTION | 1 |
| A . Hydrosilation | 1 |
| B . High Performance Liquid Chromatography (HPLC) | 2 |
| C . Silica Surface | 3 |
| D . 4-Methoxyphenol-4-Allyloxybenzoate (MPAB) As The Bonded Phase | 4 |
| CHAPTER II - EXPERIMENTAL | 6 |
| A . Chemicals | 6 |
| 1 . Chemicals For Preparing Silica Hydride | 6 |
| 2 . Chemicals For Preparing MPAB | 6 |
| 3 . Chemicals For Preparing Bonded Phase Silica | 8 |
| B . Instruments And Operating Procedures | 9 |
| 1 . Differential Scanning Calorimeter (DSC) | 9 |
| 2 . Diffuse Reflectance Infrared Fourier Transform Spectroscopy (DRIFT) And Fourier Transform Infrared Spectroscopy (FTIR) | 10 |
| 3 . Elemental Analyzer | 11 |
| 4 . High Performance Liquid Chromatography (HPLC) | 12 |
| 5 . Nuclear Magnetic Resonance (NMR) | 15 |
| C . Synthetic Procedures | 15 |
| 1 . Silica Hydride | 15 |
| 2 . Synthesis Of Organic Bonded Silica | 17 |
| a . MPAB Bonded Silica | 17 |
| b . Cholesteryl-10-Undecenoate Bonded Silica | 19 |
| 3 . Column Packing | 19 |
| CHAPTER III - RESULTS AND DISCUSSIONS | 20 |
| A . Confirmation Of MPAB Bonded On The Silica Surface | 20 |
| 1 . DSC Thermograms | 20 |
| 2 . DRIFT Spectra | 23 |
| 3 . CP-MAS ²⁹ Si NMR Spectra | 27 |
| 4 . CP-MAS ¹³ C NMR Spectra | 27 |

| | |
|--|-----------|
| B . Reaction Variables Versus Surface Coverage Of MPAB-Bonded Phase | 31 |
| 1 . Organic Bonding Material | 32 |
| 2 . Solvent For Chloroplatinic Acid Hexahydrate | 34 |
| 3 . Catalyst : MPAB Molar Ratio | 37 |
| 4 . Temperature | 39 |
| 5 . Reaction Time | 41 |
| 6 . Solvent (Toluene) Volume | 42 |
| C . Chromatographic Studies | 43 |
| 1 . Separations Of SRM 869 | 43 |
| 2 . Separations Of SRM 1647c | 50 |
| a . Isocratic Separations | 50 |
| b . Gradient Separations | 55 |
| 3 . Column Characterization | 65 |
| CHAPTER IV - CONCLUSION | 68 |
| CHAPTER V - REFERENCES | 69 |

List of Figures

| | |
|--|----|
| Figure 1. Functional Groups on the Silica Surface | 4 |
| Figure 2. The Structure of 4-Methoxyphenol-4-Allyloxybenzoate (MPAB) | 5 |
| Figure 3. The DSC Thermogram of MPAB | 21 |
| Figure 4. The DSC Thermograms of (a) MPAB-Bonded Silica versus Silica Hydride and (b) Background versus Silica Hydride | 22 |
| Figure 5. The DRIFT Spectra of (a) Native Silica and (b) Silica Hydride | 24 |
| Figure 6. The DRIFT Spectrum of MPAB | 25 |
| Figure 7. The DRIFT Spectrum of MPAB-Bonded Silica | 26 |
| Figure 8. The CP-MAS ²⁹ Si NMR Spectrum of MPAB-Bonded Silica | 28 |
| Figure 9. The CP-MAS ¹³ C NMR Spectrum of MPAB | 29 |
| Figure 10. The CP-MAS ¹³ C NMR Spectrum of MPAB-Bonded Silica | 30 |
| Figure 11. The Structure of Cholesteryl-10-Undecenoate | 32 |
| Figure 12. The FTIR Spectrum of Chloroplatinic Acid Hexahydrate in Isopentanol | 36 |
| Figure 13. Plot of Catalyst : MPAB Molar Ratios versus Surface Coverage | 38 |
| Figure 14. Plot of Temperature versus P _c | 40 |
| Figure 15. Plot of Reaction Time versus Surface Coverage | 42 |
| Figure 16. The Structures of the Components in SRM 869 | 45 |
| Figure 17. The Chromatograms of SRM 869 on (a) Monomeric-C18, (b) Oligomeric-C18 and (c) Polymeric-C18 Phases | 46 |
| Figure 18. The Chromatogram of SRM 869 on Column 1 with 85:15 ACN/Water | 47 |
| Figure 19. The Chromatogram of SRM 869 on Column 2 with 85:15 ACN/water | 48 |
| Figure 20. The Chromatograms of SRM 869 on Column 3 with 85:15 ACN/water (a) at 254 and (b) 210 nm | 49 |
| Figure 21. The Structures of the Components of SRM 1647c | 51 |
| Figure 22. The Chromatograms of SRM 1647c on Column 1 with (a) 80:20 ACN/Water and (b) 50:50 Methanol/Water | 53 |
| Figure 23. The Chromatograms of SRM 1647c on Column 2 with (a) 85:15 ACN/Water and (b) 80:20 Methanol/Water | 54 |
| Figure 24. The Chromatograms of SRM 1647c on (a) Monomeric-C18, (b) Oligomeric-C18 and (c) Polymeric-C18 Phases | 56 |
| Figure 25. The Chromatogram of SRM 1647c on Column 1 with Gradient (i) | 58 |
| Figure 26. The Chromatograms of SRM 1647c on Column 2 with (a) Gradient (i) and (b) Gradient (ii) | 59 |
| Figure 27. The Chromatograms of SRM 1647c on Column 3 with Gradient (iii) at (a) 254 and (b) 210 nm | 60 |
| Figure 28. The Chromatograms of SRM 1647c on Column 3 with Gradient (iv) at (a) 254 and (b) 210 nm | 61 |
| Figure 29. The Chromatogram of SRM 1647c on Column 1 with Gradient (vii) | 62 |
| Figure 30. The Chromatograms of SRM 1647c on Column 2 with (a) Gradient (v) and (b) Gradient (vi) | 63 |

| | |
|---|----|
| Figure 31. The Chromatograms of SRM 1647c on Column 2 with (a) Gradient (viii) and (b) Gradient (ix) | 64 |
| Figure 32. The Chromatograms of Column-Efficiency Determinations on Column 3 (a) Freshly Packed and (b) after 32.8 Hours of Operations | 66 |

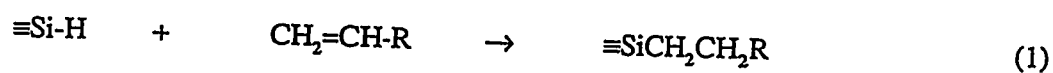
List of Tables

| | |
|--|----|
| Table 1 - The CAS Registry Number of Chemicals Used | 7 |
| Table 2 - Matrices of Chromatographic Samples (1 ml Total Volume) | 14 |
| Table 3 - The Surface Coverages of MPAB- and Cholesteryl-10-Undecenoate-Hydrosilations | 33 |
| Table 4 - The Formula Weights and the L/B Ratios of the SRM 1647c Analytes | 52 |
| Table 5 - Gradient Conditions Employed for the Study of SRM 1647c | 57 |

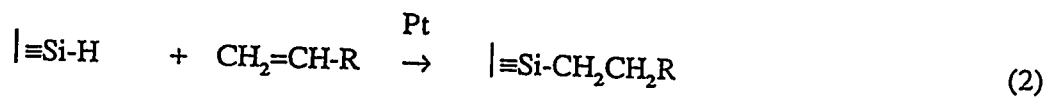
Chapter I - Introduction

A . Hydrosilation

In 1957, Speier *et al.* [1] first published a hydrosilation reaction between liquid silanes and liquid terminal olefins *via* various platinum catalysts.



Among all platinum catalysts, Speier *et al.* concluded that chloroplatinic acid hexahydrate dissolved in isopropanol was the most active. In subsequent years, this catalyst has been widely used and is named as "Speier's catalyst" [2]. Applying the concept of homogenous hydrosilation, Sandoval and Pesek [3] successfully bonded 1-octene and 1-octadecene onto a pretreated silica surface.



This breakthrough is important to liquid-chromatographic studies because other hydrocarbon-silica reactions either are difficult to control or result in significant loss of bonded hydrocarbon [3] (or referred to as column bleeding). Heterogeneous hydrosilation enables terminal olefins to be bonded easily onto the solid support for chromatographic separation.

B . High Performance Liquid Chromatography (HPLC)

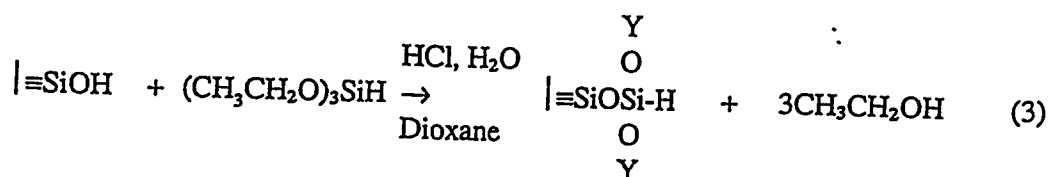
Early column chromatographic separation took place in glass columns of 1 to 5 cm in diameter and 50 to 500 cm in length. The diameter of the solid particles packed inside the column was between 50 to 200 μm . Separation usually required several hours. Attempts to reduce the separation time were often accompanied by lower column efficiency. Later, by packing 3- to 10- μm particles in smaller columns, the efficiency was improved. This new technology is named as high performance liquid chromatography (HPLC) [4].

Reverse-phase HPLC receives more attention than normal-phase HPLC because it resolves most biological, pharmaceutical and environmental mixtures. The mobile phase in reverse-phase chromatography is a polar mixture of organic solvent(s) and water. The stationary phase is composed of non-polar hydrocarbons, which are either physically adsorbed or chemically bonded to an inert solid support. In order to attain a reasonable flowrate, the mobile phase, together with the analyte(s), are pushed through the column at high pressures (around 500 to 1000 psi). Physical adsorption of the hydrocarbons on the support will result in severe column bleeding. Consequently, chemical bonding is preferred. Besides silica, alumina, zirconia, polymer derivatives and other solid supports are available. Among all these supports, silica is the most popular because its surface chemistry has been studied the most. Silica is also spherical and mechanically sturdy, which is ideal for uniform column-packing. The porous structure of silica allows larger analyte-stationary phase interaction. Therefore, silica was chosen as the solid support for this research.

C . Silica Surface

A siloxane ($\equiv\text{Si-O-Si}\equiv$) network makes up the basic structure of the native silica (native silica refers to the silica before any surface modification). On the silica surface, silicon atoms are bonded to various forms of hydroxide groups (Figure 1). These hydroxide groups are significantly more reactive than the siloxane network. Hence, they are the primary sites for surface modifications. However, these reactive hydroxides ($\text{pK}_a = 5$ to 7) [5] can attract polar solutes by hydrogen-bonding or dipole-dipole interaction. This situation will result in tailing peaks for these polar analytes in reverse-phase chromatography. As a result, one of the goals of most surface reactions is to eliminate these hydroxides from the silica surface. However, around $8 \pm 1 \mu\text{mol}/\text{m}^2$ of hydroxides [5] are found on the surface. Even after surface reactions, due to steric hindrance between the bonded hydrocarbons, some hydroxides still remain. For example, the maximum bonding density of the octadecyl (C18) alkane is $4.5 \mu\text{mol}$ of C18/ m^2 [5] on the surface (usually referred to as surface coverage).

To reduce the number of unreacted silanols, as well as to provide hydride groups for the hydrosilation reaction, Chu *et al.* [6] suggested a triethoxysilane (TES) surface modification (equation 2) to create a new hydride-bearing layer for the heterogeneous hydrosilation.



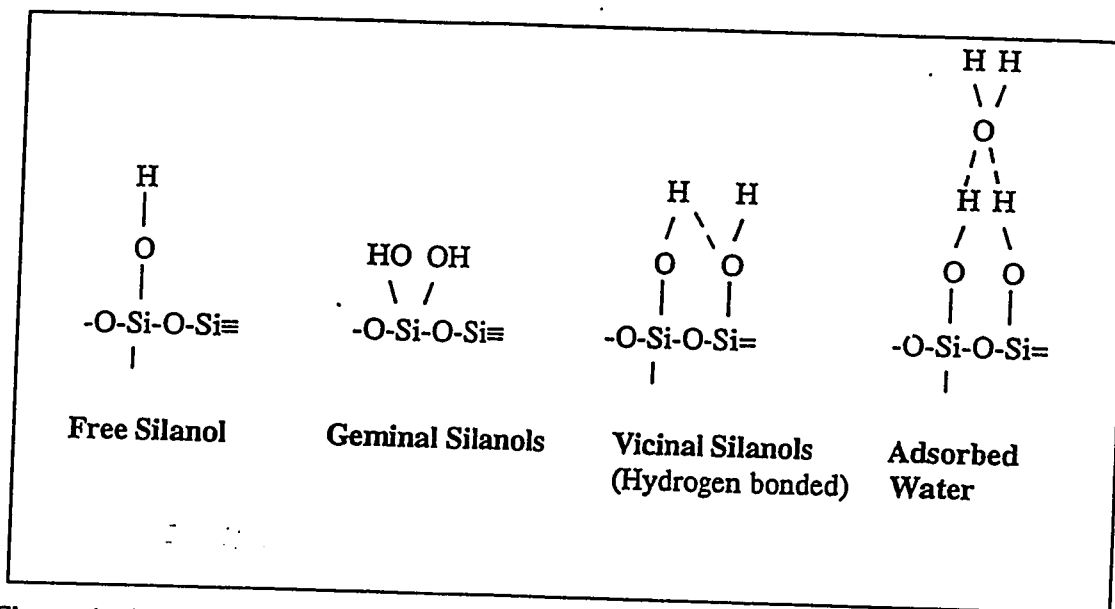


Figure 1. Functional Groups on the Silica Surface

The Y represents either a hydrogen, or another silicon atom on the surface. The ^{29}Si cross-polarization (CP) NMR shows that 90% of the hydride-bearing silicons formed three siloxane linkages with their neighboring silicons [3]. This is desirable because 90% of the bonded hydrocarbons are less likely to be cleaved off from the silica surface. Thus, column bleeding is reduced. Consequently, hydrosilation on a TES-treated silica surface has been chosen as the best hydrocarbon-silica reaction approach for this research.

D. 4-Methoxyphenol-4-Allyloxybenzoate (MPAB) As The Bonded Phase

To carry out equation 2, besides a silicon-hydride bearing surface, a terminal olefin is necessary. MPAB (Figure 2) was selected because the MPAB-silica hydrosilation has

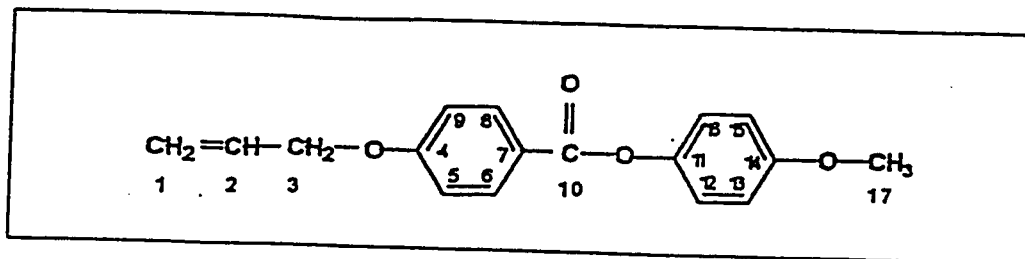


Figure 2. The Structure of 4-Methoxyphenol-4-Allyloxybenzoate (MPAB)

been proven successful [7]. Its molecular structure is rather linear, such that the low steric hindrance between adjacent MPAB molecules produces a high surface-coverage bonded silica. Hence, the chromatographic selectivity is enhanced [8, 9].

Furthermore, the chromatographic properties of the MPAB-bonded stationary phase have not been extensively studied. A preliminary chromatographic study [10] shows that the MPAB stationary phase resolves phenanthrene and anthracene (structural isomers) better than C18 phases. Also a phase transition is observed when homologues of alkylarylketones were separated on the MPAB stationary phase. Similar phenomena are observed on the polymeric C18 phases when separating homologues of other groups [11]. In this research, the chromatographic studies were focused on characterizing the molecular alignment and the retention mechanism of the MPAB stationary phase in comparison with the conventional C18 phases. Finally, the column efficiency of the MPAB phase was determined.

Chapter II - Experimental

A . Chemicals

The CAS registry numbers of all chemicals used in chapter II are listed in Table 1.

1 . Chemicals For Preparing Silica Hydride

The native silica--Vydac 101TP (particle diameter-6.5 μ m, pore diameter-380 Å, specific surface area-106.5 m²/g)--was a gift from the Separations Group (Hesperia, CA, USA). 1,4-Dioxane (< 0.05% water, Eastman, Rochester, NY, USA) was purified by distillation (the first 10% of the distillate was discarded; the rest was stored in a dry glass bottle). Concentrated hydrochloric acid was obtained in reagent grade. Triethoxysilane was purchased from Huls America Incorporated (Bristol, PA, USA). Tetrahydrofuran (anhydrous, 99%) was purchased from Aldrich (Milwaukee, WI, USA). Diethyl ether (anhydrous) was obtained from Fisher Scientific (Fair Lawn, NJ, USA).

2 . Chemicals For Preparing MPAB

MPAB was synthesized according to a procedure from M. A. Apfel *et al.* [12]. 4-Methoxyphenol (99%), pyridine (99+%) and allyl bromide (either 97 or 99%) were purchased from Aldrich. 4-Hydroxybenzoic acid, *N,N*-dimethylformamide, potassium

hydroxide and methanol were obtained in reagent grade. Ethanol (200 proof) was purchased from Goldshield Chemical Company (Hayward, CA, USA). Thionyl chloride (reagent grade) was obtained from Fisher Scientific.

Table 1 - The CAS Registry Number of Chemicals Used

| Chemical Name | CAS Registry Number |
|--|---------------------|
| Acenaphthene | [83-32-9] |
| Acenaphthylene | [208-96-8] |
| Acetanilide | [103-84-4] |
| Acetonitrile | [75-05-8] |
| Allyl bromide | [106-95-6] |
| Anthracene | [120-12-7] |
| Benz[<i>a</i>]anthracene | [56-55-3] |
| Benzo[<i>a</i>]pyrene | [50-32-8] |
| Benzo[<i>b</i>]fluoranthene | [205-99-2] |
| Benzo[<i>ghi</i>]perylene | [191-24-2] |
| Benzo[<i>k</i>]fluoranthene | [207-08-9] |
| Calcium chloride | [10043-52-4] |
| Cholesteryl-10-undecenoate | [30948-01-7] |
| Chloroform | [67-66-3] |
| Chloroplatinic acid hexahydrate | [16941-12-1] |
| Chrysene | [218-01-9] |
| Cyclohexanone-2,4-dinitrophenylhydrazone | [1589-62-4] |
| Dibenz[<i>a,h</i>]anthracene | [53-70-3] |
| Diethyl ether | [60-29-7] |
| 7-(2,3-Dihydroxypropyl)theophylline | [479-18-5] |
| <i>N,N</i> -Dimethylformamide | [68-12-2] |
| 1,4-Dioxane | [123-91-1] |
| Drierite | [7778-18-9] |
| Ethanol | [64-17-5] |
| Fluoranthene | [206-44-0] |
| Fluorene | [86-73-7] |
| Hydrochloric acid | [7647-01-0] |
| 4-Hydroxybenzoic acid | [99-96-7] |

| | |
|--|--------------|
| Indeno[1,2,3- <i>cd</i>]pyrene | [193-39-5] |
| Indium | [7440-74-6] |
| Isopropanol | [67-63-0] |
| Methanol | [67-56-1] |
| 4-Methoxyphenol | [150-76-5] |
| 4-Methoxyphenol-4-allyloxybenzoate | [73376-32-6] |
| Isopentanol | [123-51-3] |
| Methylene chloride | [75-09-2] |
| Molecular sieves, 5A | [69912-79-4] |
| Naphthalene | [91-20-3] |
| Phenanthrene | [85-01-8] |
| Phenanthro[3,4- <i>c</i>]phenanthrene | [187-83-7] |
| Potassium bromide | [7758-02-3] |
| Potassium hydroxide | [1310-58-3] |
| Potassium nitrate | [7757-79-1] |
| Pyrene | [129-00-0] |
| Pyridine | [110-86-1] |
| 1,2:3,4:5,6:7,8-Tetrabenzonaphthalene | [191-68-4] |
| Tetrahydrofuran | [109-99-9] |
| Thionyl chloride | [7719-09-7] |
| Toluene | [108-88-3] |
| Triethoxysilane | [998-30-1] |
| Xylenes, mixed | [1330-20-7] |

3. Chemicals For Preparing Bonded Phase Silica

Cholesteryl-10-undecenoate was purchased from Sigma (St. Louis, MO, USA). Methylene chloride, toluene and isopropanol were obtained in reagent grade. Toluene was dried by stirring in anhydrous calcium chloride (mesh 8, Fisher Scientific) and purified by distillation as follows: first 1 L of toluene was stirred with 5 g of anhydrous calcium chloride overnight. During distillation, 1 g of type 5A molecular sieves (Matheson Coleman & Bell, Norwood, OH, USA) was placed in the receiving flask. Afterwards, the distillate was stored with another 10 g of type 5A molecular sieves in a dry glass bottle.

The distilled toluene was used in all subsequent syntheses and washing steps. Isopentanol was obtained from J.T. Baker (Phillipsburg, NJ, USA). Isopropanol (reagent grade) was dried according to reference 13. Chloroplatinic acid hexahydrate (99.9%) was ordered from Strem Chemical (Newburyport, MA, USA). The catalyst solution was prepared as follows: chloroplatinic acid hexahydrate was weighed out quickly on an analytical balance (Mettler AE 200, Mettler Instrument Corp., Hightstown, NJ, USA) according to the concentration desired. It was then transferred to a volumetric flask, dissolved and diluted to the mark by isopentanol.

B . Instruments And Operating Procedures

1 . Differential Scanning Calorimeter (DSC)

The differential scanning calorimetry set-up includes a calorimeter (Perkin-Elmer DSC 7, Perkin-Elmer, Norwalk, CT, USA), an instrument controller (Perkin-Elmer TAC 7) and a plotter (Hewlett-Packard 7475A, Hewlett-Packard, Palo Alto, CA, USA). Compressed nitrogen or oxygen was filtered through a gas purifier (model 461, Matheson Product Inc., Seaucus, NJ, USA) before entering the sample compartment. A flow meter (Matheson 7261(A)) was installed to adjust the gas flow. Aluminum sample pans were used for heat-flow measurement below 550°C. For all other cases, platinum sample pans were used. The baseline was obtained by scanning an empty sample pan within the desired temperature range. This signal was subtracted off in all subsequent reference and sample

runs. Indium, provided by Perkin-Elmer, served as a reference. A temperature correction factor was determined by subtracting the measured from the true transition temperature of indium. Then the measured transition temperature of each sample was adjusted according to this factor to determine the “real” transition temperature. Generally, samples between 0.5 to 30 mg were used. They were weighed out on an electro-microbalance (Cahn 4700-automatic; Cerritos, CA, USA).

2 . Diffuse Reflectance Infrared Fourier Transform Spectroscopy (DRIFT) And Fourier Transform Infrared Spectroscopy (FTIR)

Liquid nitrogen was used to supply gaseous nitrogen (55-65 psi) to the sample compartment of the infrared spectrophotometer (Perkin-Elmer model 1800) to drive away moisture. For the FTIR analyses, liquid samples were immobilized in between potassium chloride plates and were referenced to empty potassium chloride plates. Double-beam FTIR spectra were scanned at a 2-cm^{-1} resolution and a 0.7 noise level. The infrared spectra of solid silica samples were taken by the diffuse-reflectance technique. The diffuse-reflectance accessory (Spectra Tech., Stamford, CT, USA) consists of a 2-mm diameter and 2-mm depth sample cup. One part of a silica sample was mixed with ten parts of ground IR-grade potassium bromide (99.5%, Spectrum, Gardena, CA, USA) by weight. After the sample cup was filled with this mixture, the top was smoothed down by a glass plate. The reflectance signal of the sample was compared against that of pure

potassium bromide. Each spectrum was scanned 100 times at a resolution of 2 cm⁻¹. Both DSC and DRIFT shared the same computer system (Perkin-Elmer model 7500).

3 . Elemental Analyzer

The elemental analyzer measures the relative composition of carbon, nitrogen and hydrogen of a sample. First, a sample is combusted between 950 to 1000°C. Mainly carbon dioxide and water are produced. The carbon and hydrogen contents are detected by comparing the difference in thermal conductivity before and after the removal of each product. Since nitrogen is also oxidized to various forms of oxides during combustion, to ensure an accurate determination of the nitrogen content, nitrogen oxides are reduced to nitrogen between 650 to 700°C before the thermal conductivity measurements.

The elemental analyzer (Perkin-Elmer 240C) was connected to a chart recorder (Perkin-Elmer 56-3003) for the output. High-purity (grade 4.7) compressed helium and oxygen were supplied to the analyzer at 15-20 and 25-30 psi respectively. Either acetanilide or cyclohexanone-2,4-dinitrophenylhydrazone from Perkin-Elmer served as a calibration standard. 7-(2,3-dihydroxypropyl)theophylline (99%) from Aldrich was used for instrument certification. Samples between 1 to 3 mg were weighed out on the Cahn electro-microbalance. All determinations were performed in triplicate.

The surface coverage, α_R , of the bonded silica was calculated as follows [14]:

$$\alpha_R (\mu\text{mol}/\text{m}^2) = \frac{10^6 P_c}{(100M_{c,n_c} - P_c M_R) S} \quad (4)$$

where P_c is the carbon-percentage difference in the modified silica and the silica hydride, n_c refers to the number of carbon atoms on the skeleton of the hydrocarbon for bonding, M_c and M_R represent the atomic weight of a carbon atom and the formula weight of the bonded hydrocarbon respectively and S (m^2/g) is the specific surface area of the native silica as determined by the Brunauer, Emmet and Teller (BET) nitrogen adsorption method performed at the Chevron Research Center, Richmond, CA.

4. High Performance Liquid Chromatography (HPLC)

The Model 1050 HPLC system from Hewlett-Packard (Palo Alto, CA, USA) consists of a quaternary pump, a multi-wavelength absorbance detector, an autosampler, and a solvent tray. This HPLC system was controlled by an HP Vectra 05/20 computer with a Video Graphics Color display monitor, *via* an HP 35900 Interface equipment. The chromatographs were printed on an HP DeskJet Plus printer. Compressed helium at about 50 ml/min was used to degas the organic solvents and water for the first 15 minutes. Then the helium flow was kept at about five ml/min while the mobile phase was pumped through the column. Compressed air between 10 to 30 psi was required to operate the autosampler. All chromatographic separations were run at less than 100 bar of back pressure and less than $\pm 2\%$ of ripple. Ripple reflects the synchronization between the piston and the exit valve of the first pump. The piston rate or the compressibility of the mobile-phase mixture must be adjusted when the ripple is greater than $\pm 2\%$.

Methanol-water, acetonitrile (ACN)-water and tetrahydrofuran (THF)-water mixtures were the mobile phases for the chromatographic separations. Methanol and acetonitrile were reagent grade. THF was HPLC grade (Burdick & Jackson Laboratories, Inc., Muskegon, MI, USA). Distilled water was purified by a Milli-Q[®] system (Millipore Corporation, Bedford, MA, USA) to remove particulates and ions. All solvents and water were then filtered through a 0.20- μ m nylon membrane before being used as mobile phases. The polyaromatic-hydrocarbon (PAH) mixtures (SRM 1647c and SRM 869) were obtained from the National Institute of Standards and Technology (Gaithersburg, MD, USA). The dead time of the HPLC instrument was determined by the retention time of high-purity potassium nitrate. With a flow of one ml/min, potassium nitrate eluted at around 1.10 minutes. Samples for individual peak identification of the SRM 1647c separation were prepared from high-purity naphthalene, phenanthrene, anthracene, fluorene, pyrene and dibenz[*a,h*]anthracene according to Table 2. Injection samples were kept in sample vials sealed by a crimper. To ensure a precipitate-free sample, ultrasonication by an ultrasonic cleaner (Branson 2200, Branson Ultrasonics Corporation, Danbury, CT, USA) was used to break up small particulates. The crimper, sample vials and caps, nylon membrane and the filtration set-up were purchased from Alltech, Deerfield, IL, USA.

After packing the bonded silicas into stainless-steel tubes (0.25 inches OD, 4.6 mm X 150 mm, Alltech), all columns were equilibrated with pure methanol. To switch from methanol to the desired mobile-phase composition for separation, the composition was

changed in increments of 5% by volume after the back pressure and the ripple were stabilized. When a column had been used for a long time, a 10% volume change per minute was used for switching between mobile-phase compositions. If a column was not used for several days, the solvent was switched back to pure methanol by incremental change in the mobile-phase composition.

Table 2 - Matrices of Chromatographic Samples (1 ml Total Volume)

| Analyte | Potassium Nitrate (12.2 mM) | Organic Solvent | Water |
|---|--------------------------------|-----------------|-------|
| 10µl of 18.2 mM naphthalene in ACN | 20 µl | 340µl ACN | 630µl |
| 10µl of 16.8 mM phenanthrene in ACN | 20 µl | 340µl ACN | 630µl |
| 10µl of 37.4 mM fluorene in ACN | 20 µl | 340µl ACN | 630µl |
| 10µl of 19.9 mM pyrene in ACN | 20 µl | 340µl ACN | 630µl |
| 980µl of 4.4 mM chrysene in ACN | 20 µl | | |
| 980µl of 5.6 mM anthracene in ACN | 20 µl | | |
| 980µl of 3.6 mM dibenz[a,h]-anthracene in ACN | 20 µl | | |
| 100µl of SRM | 20 µl | 900µl ACN | |

| | |
|--------------------|-----------|
| 1647c in methanol | |
| 100 μ l of SRM | 2 μ l |
| 869 in methanol | |

5. Nuclear Magnetic Resonance (NMR)

The ^{13}C and ^{29}Si NMR spectra were obtained on a Bruker MSL 300 spectrometer. CP and magic-angle spinning (MAS) techniques were employed to enhance the signal-to-noise ratio. Solid samples, spinning at 4700-5200 Hz, were placed in ZrO_2 double bearing rotor. External glycine and polyhydridosiloxane samples were served as the references for the ^{13}C and ^{29}Si analyses respectively. Pulse widths of 6.5 and 5.0 μsec were used for the ^{13}C and ^{29}Si spectra respectively. Both analyses were operated at a 5-msec contact time and a 5-sec repetition rate; the probe temperature was 20 ± 2 $^\circ\text{C}$.

C. Synthetic Procedures

1. Silica Hydride

Polymerization of TES occurs in the presence of moisture. Therefore, a 125-ml pressure-equalizing-addition funnel, a 50.00 ml volumetric flask and a 10-ml graduated cylinder were dried in an oven overnight at 110 $^\circ\text{C}$. The preparation of a 1.00 M TES solution was performed in a nitrogen-filled glove box. Once the glassware was removed

from the oven, it was greased and quickly placed in the glove box. The box's opening was then sealed with a plastic diaphragm and the box was purged alternatively by nitrogen and vacuum five times. The last nitrogen purge was barely enough to fill the box. TES (9.6 ± 0.1 ml) was measured out in the 10-ml graduated cylinder and transferring it to the 50.00 ml volumetric flask. The volume was brought to the mark by distilled 1,4-dioxane. The 1 M TES solution was then transferred to the pressure-equalizing-addition funnel. Outside the glove box, the funnel was connected to a side-neck of a 500-ml, three-necked round-bottom flask. Then 11.1 ± 0.05 g of Vydac 101TP silica, 273 ± 0.5 ml of distilled 1,4-dioxane (see page 6) and 10.8 ± 0.05 ml of 2.3 M hydrochloric acid were transferred to the reaction flask containing a 0.5-in magnetic stir-bar.

A condenser, with a Drierite (8-mesh, W.A. Hammond Drierite Company, Xenia, OH, USA)-filled drying tube on top, was positioned in the middle neck of the flask. A thermometer with an adapter were placed in the third opening. The mixture was stirred and heated to reflux, followed by dropwise addition of TES (about two drops per minute) for 25 to 30 minutes. The solution was then heated at reflux for one hour.

When the reaction was finished, the joints were degreased with mixed xylenes. The mixture was allowed to settle and the liquid phase was decanted. The silica hydride paste was divided into four equal parts in four centrifuge tubes. The solid was recovered by centrifugation for 10 minutes at 1500 rpm (model HN-S, DAMON/IEC Division, Needham Heights, MA, USA). The supernatant was decanted. A freshly-prepared 1:1 THF-deionized water (by volume) solvent was poured into the centrifuge tubes to about

half the height. The silica hydride in the THF-water solvent were stirred for 10 minutes. The mixture was centrifuged again for 10 minutes. The solid phase was washed and centrifuged three more times with a 1:1 volume ratio of THF-deionized water, two times with pure THF and two times with diethyl ether.

After all washing and centrifugation, the silica hydride was transferred to a recrystallization dish by a spatula. The dish was covered by a Speedy-Vap watch-glass. The silica hydride was dried in the hood at room temperature overnight, followed by drying in an oven at 110°C overnight. Finally, the product was characterized by elemental analysis, DSC, NMR and DRIFT.

2. Synthesis Of Organic Bonded Silica

a . MPAB Bonded Silica

The catalyst solution is moisture-sensitive. Therefore, chemical addition and glassware assembly were performed in a nitrogen-filled glove box. All glassware was dried in an oven at 110 °C overnight. Under ambient conditions, a 25-ml, three-necked round-bottom flask was removed from the oven and was cooled down to about 60 °C, while 0.1720 ± 0.0002 g of MPAB was weighed out on a Mettler analytical balance. Then the MPAB was transferred to the cooled flask. Together with other greased glassware and chemicals, the 25-ml round-bottom flask were quickly placed in the glove box. The glove box was purged with nitrogen as described on page 16. Distilled toluene ($6.2 \pm$

0.05 ml) from page 8 was measured out in a 10-ml graduated cylinder and added to the round-bottomed flask. Finally, $943 \pm 0.1 \mu\text{l}$ of 8×10^{-4} M chloroplatinic acid hexahydrate in isopentanol was pipetted into the round-bottomed flask. A thermometer with an adapter, a condenser with a filled drying tube and a glass stopper were assembled on the necks of the reaction flask. The set-up was removed from the glove box. The reactants were stirred by a 0.5-in magnetic stir bar and heated to $70 \pm 2 \text{ }^\circ\text{C}$ for a one-hour induction period. Silica hydride ($0.40 \pm 0.01 \text{ g}$) was added slowly through a bent glass tube to the reactants. Afterwards, the mixture was heated to $100 \pm 2 \text{ }^\circ\text{C}$ for 48 hours.

When the reaction was over, the joints were degreased with mixed xylenes. The solution was poured into a 16 x 125 mm glass tube and centrifuged for 5 minutes. The supernatant was decanted. The solid phase was stirred for 5 minutes with toluene and centrifuged for another 5 minutes. The solid was stirred and centrifuged three more times with toluene, two times with methylene chloride and two times with diethyl ether. The last ether stirring was not centrifuged. Instead the solution was poured directly into a Whatman #50 filter paper in a Buchner funnel. The bonded silica that remained on the glass wall was scraped gently with a glass rod. The Buchner funnel was covered with a Kimwipe and suctioned by vacuum overnight.

b . Cholesteryl-10-Undecenoate Bonded Silica

A similar procedure was carried out as in section 3.a. for bonding cholesteryl-10-undecenoate to silica hydride, except the reactant matrix was different. Cholesteryl-10-undecenoate (0.42 ± 0.05 g) was reacted with 0.50 ± 0.05 g of silica hydride in 7.6 ± 0.1 ml of toluene. The hydrosilation was catalyzed by 22.8 ± 0.2 μ l of 8×10^{-4} M chloroplatinic acid hexahydrate in isopropanol.

3 . Column Packing

Various bonded silicas were packed into stainless steel columns by Dr. Eric Williamsen for chromatographic analyses. Methanol, filtered through a 0.2- μ m nylon membrane, was used as the driving solvent. Approximately 1.80 to 1.85 g of bonded silica was stirred with 10% (v/v) methanol in chloroform, followed by a 10-minute sonication. The slurry was added to the reservoir. The liquid level was brought up to the top by filtered methanol. The mixture in the reservoir was packed into the column by nitrogen under approximately 6000 psi pressure. The column remained with the packer for at least 30 minutes.

Chapter III - Results And Discussions

A . Confirmation Of MPAB Bonded On The Silica Surface

Hydrosilations were carried out as described on page 17. The products were characterized by DSC, DRIFT, ^{13}C and ^{29}Si NMR, and carbon analyses.

1 . DSC Thermograms

The pure MPAB shows a sharp thermal transition at 89.4 °C (Figure 3). On the other hand, after hydrosilation, the MPAB-bonded silica's transition occurred around 125 °C (Figure 4a). In addition, this thermal transition was broader and shifted upward because, unlike the pure MPAB, the bonded silica behaves like a heterogeneous mixture of a pure compound and an impurity. In any case, to confirm if the transition of the bonded silica was caused by MPAB, a thermal study was carried out on the silica hydride before the MPAB-hydrosilation (Figure 4a). The sample weights of the MPAB-bonded silica and the silica hydride differed only by 0.2 mg to allow direct comparison of the thermograms. Heat was absorbed by the silica hydride from 55 to 160 °C. The maximum occurred at around 100 °C. The sudden rise in heat flow observed in both the thermograms of silica hydride and bonded silica between 50 and 55 °C was caused by a drop in the initial background signal (Figure 4b). Overall, the transition pattern before and after hydrosilation is similar. As a result, calorimetry is unable to confirm the success of the

hydrosilation reaction because of the possible interference from silica hydride and the low weight percent of MPAB on the bonded silica.

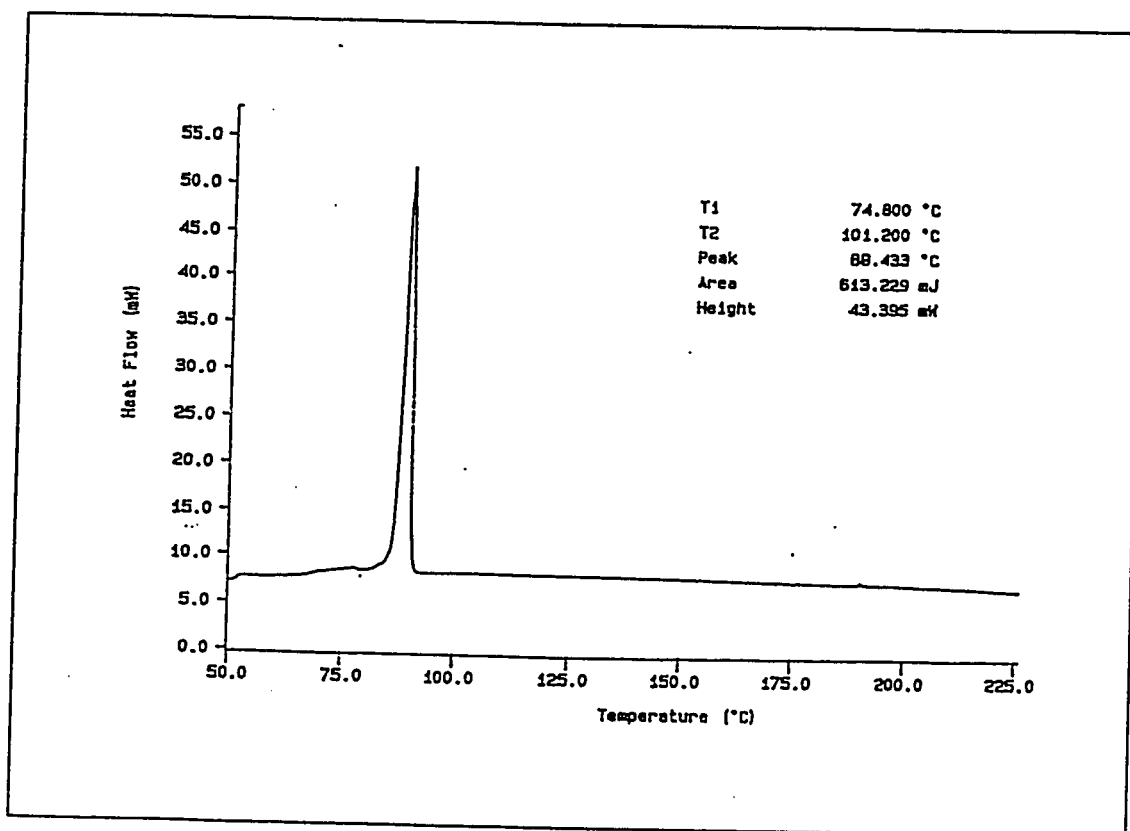


Figure 3. The DSC Thermogram of MPAB

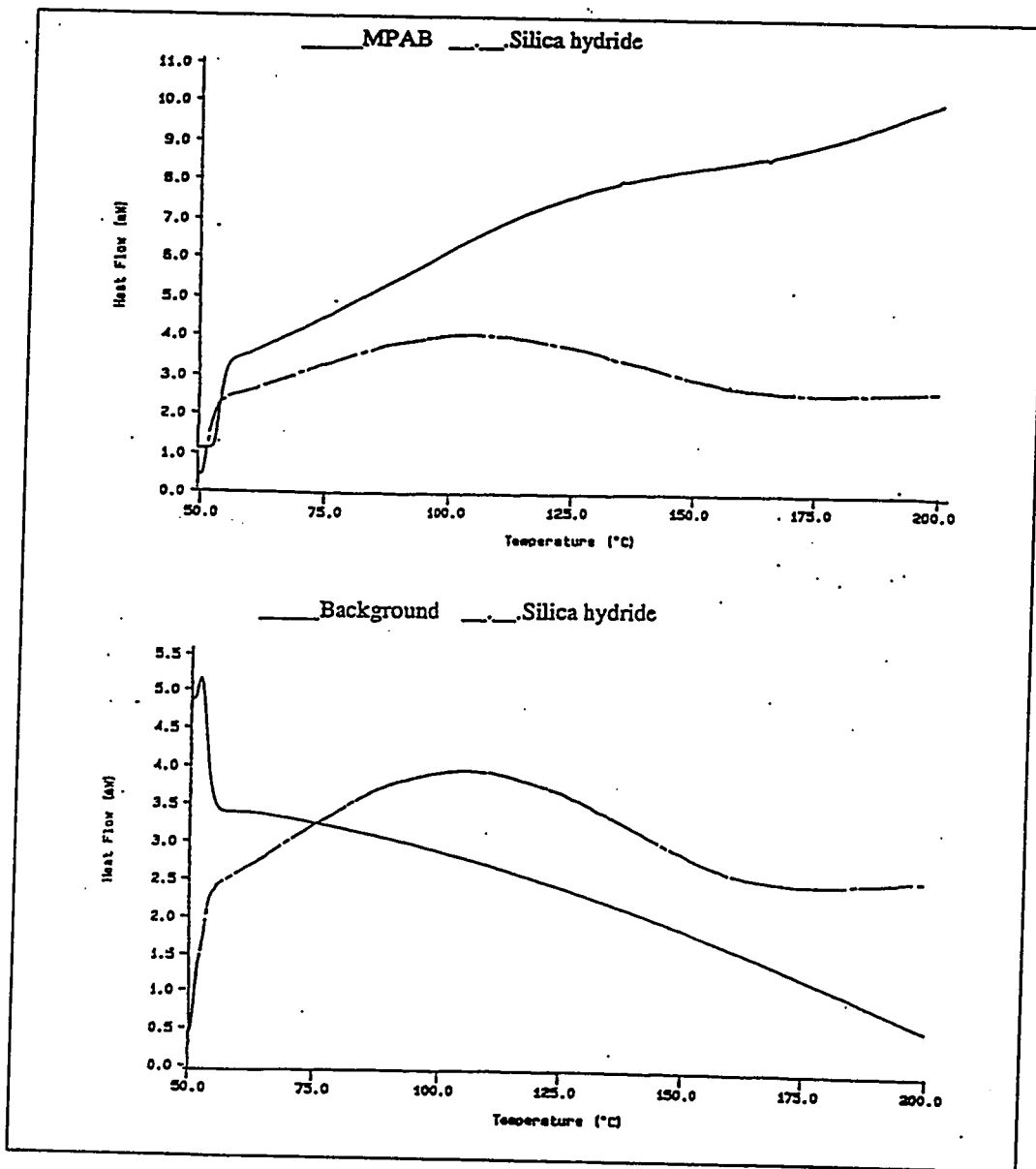


Figure 4. The DSC Thermograms of (a) MPAB-Bonded Silica versus Silica Hydride and (b) Background versus Silica Hydride

2. DRIFT Spectra

After the triethoxysilane surface modification with the native silica (equation 3), a new siloxane layer containing surface hydride groups are produced on the silica. The success of this reaction is proven by the emergence of the silicon-hydride band at 2250 cm^{-1} [3] in the DRIFT spectrum of the modified silica (Figure 5b) as compared to that of the native silica (Figure 5a). The pore structure of silica and the steric hindrance of the new hydride-bearing siloxane network may prevent all hydroxides from reacting with TES. Therefore, the hydroxide peak at 3440 cm^{-1} is still observed. Surface-adsorbed water is identified at 1620 cm^{-1} [15]. The stretching signals at 2920 and 3000 cm^{-1} [15] indicate the presence of surface-adsorbed organic solvents. Only the 1880 cm^{-1} peak was not assigned.

Apparently, the triethoxysilane modification on the native silica did not affect this feature because the peak intensity is comparable between the native and the modified silica.

The DRIFT spectrum in Figure 6 displays the key features of MPAB. The terminal olefinic C-H stretches at 3095 and 3040 cm^{-1} and the corresponding C-H bending occurs at 1410 , 980 and 910 (missing) cm^{-1} . The C-H stretch of the aliphatic alkane takes place between 2962 and 2853 cm^{-1} . The ester group stretches at 1740 cm^{-1} . The C-H stretches of the aromatic carbons are found at 1610 , 1570 , 1500 and 1450 cm^{-1} . The C-O band of the methoxy group vibrates at 1110 cm^{-1} [15]. After hydrosilation, new features are observed in the spectrum of the MPAB-bonded silica (Figure 7): 1720 cm^{-1} (ester), 1610 , 1580 , 1500 and 1450 cm^{-1} (aromatic carbons). Furthermore, the signal of the aliphatic

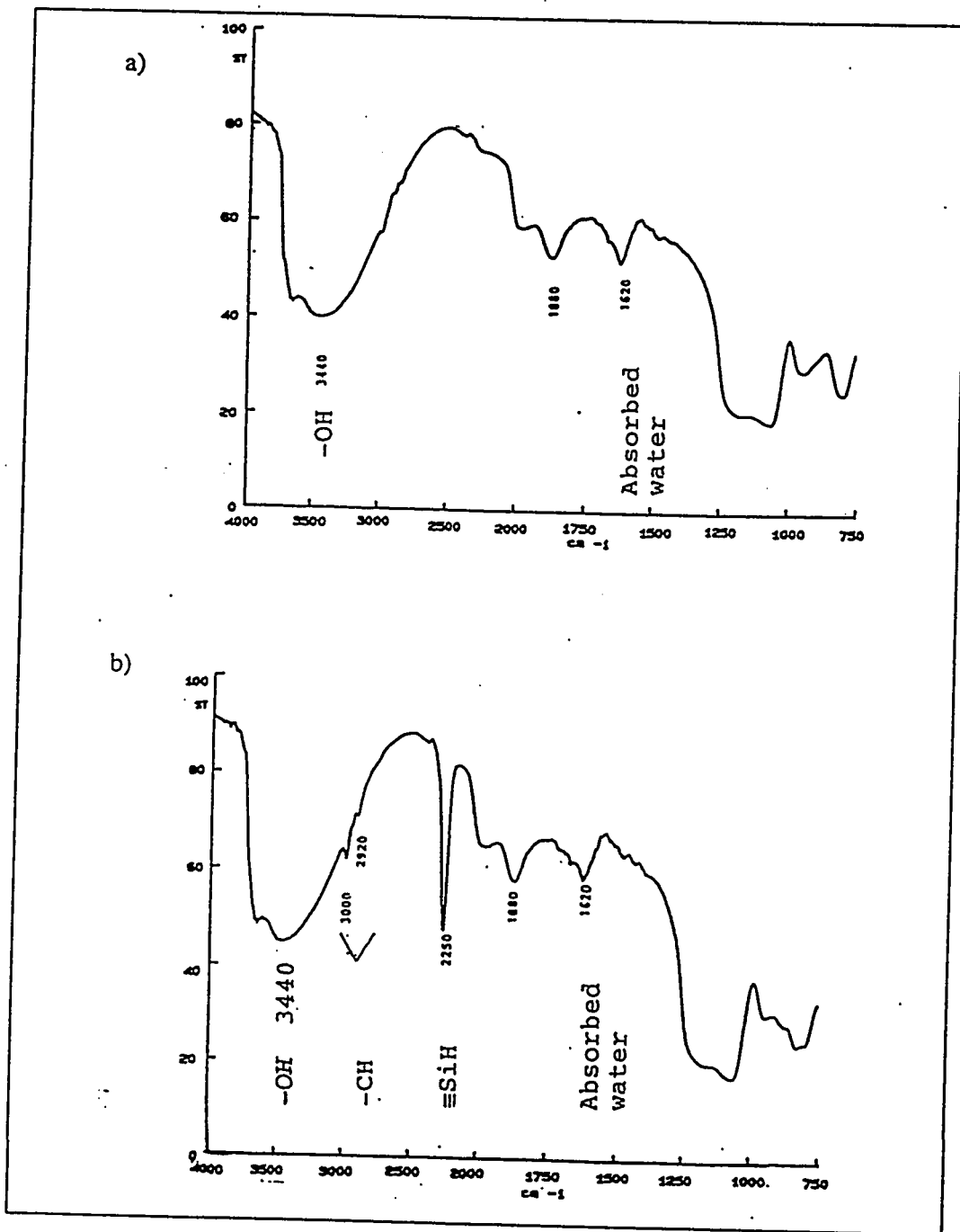


Figure 5. The DRIFT Spectra of (a) Native Silica and (b) Silica Hydride

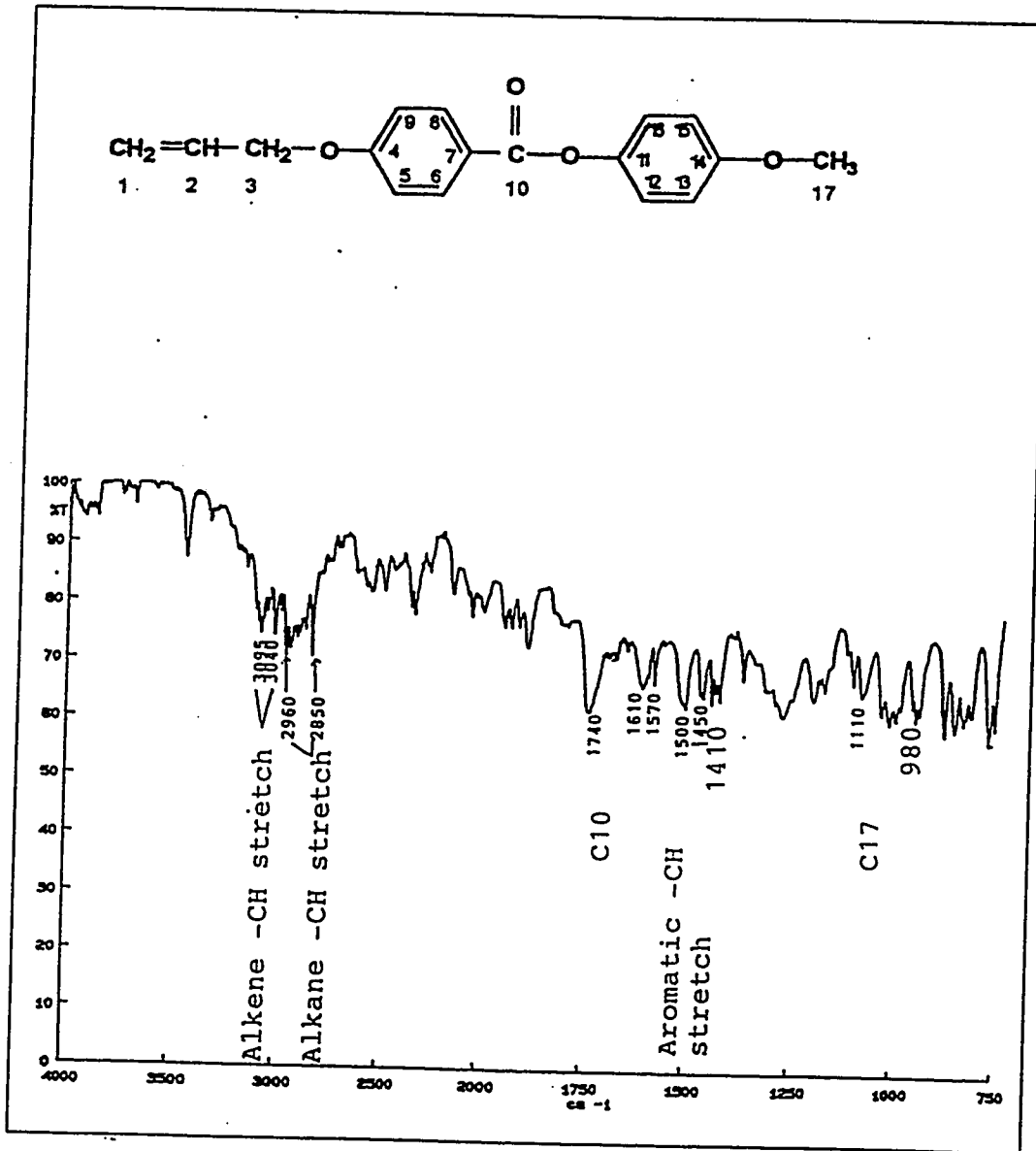


Figure 6. The DRIFT Spectrum of MPAB

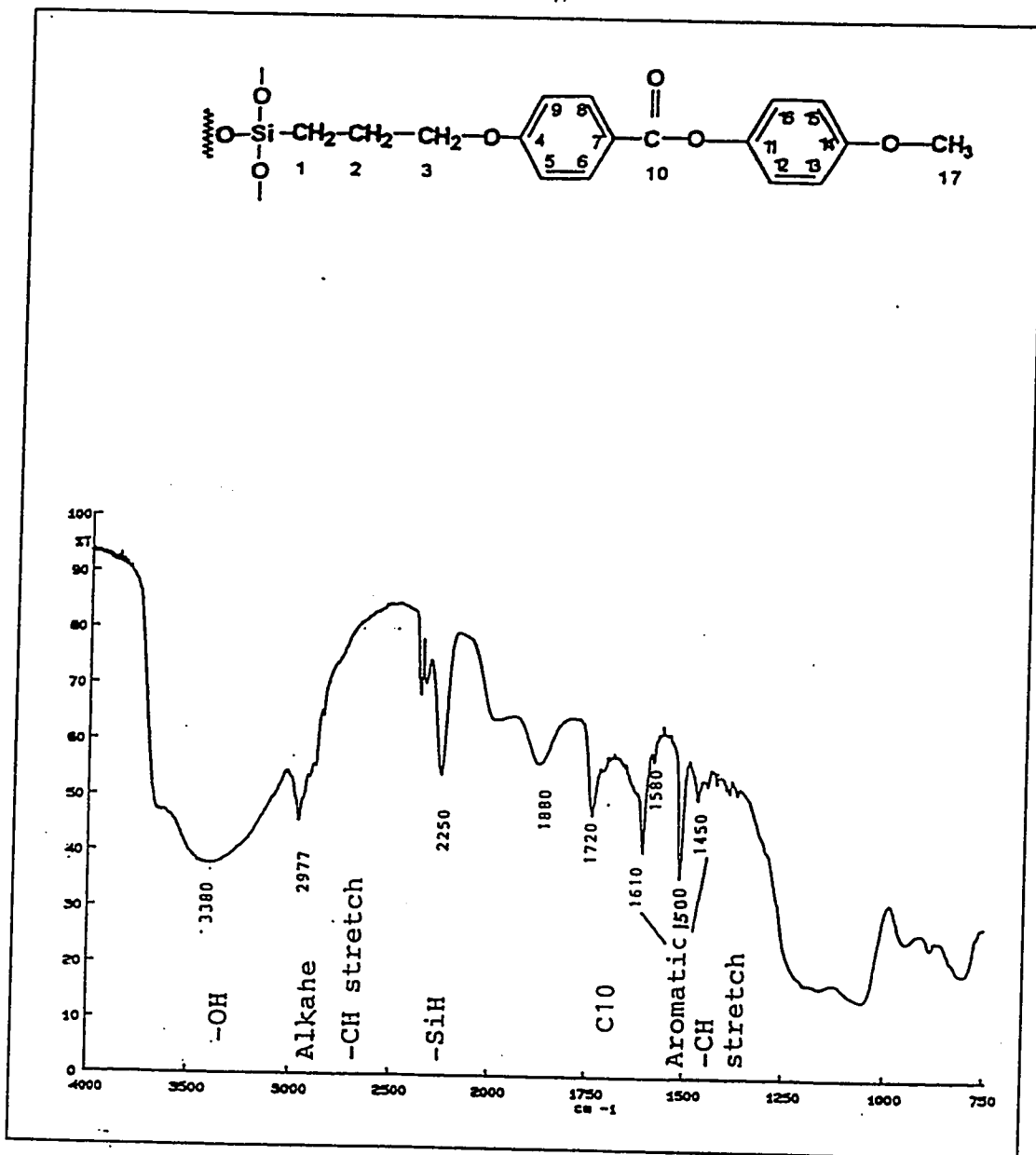


Figure 7. The DRIFT Spectrum of MPAB-Bonded Silica

alkane C-H stretch ($\sim 2977\text{ cm}^{-1}$) was enhanced. Some surface silicon-hydride groups are still present because the three-dimensional structure of the bonded MPAB prevents free MPAB from accessing these hydrides. However, all the essential IR features of the MPAB observed in Figure 7 indicate the presence of MPAB bonded to the silica surface.

3. CP-MAS ^{29}Si NMR Spectra

The CP-MAS ^{29}Si NMR (Figure 8) also reveals that the silicon-hydroxide and -hydride groups are present on the silica surface after the MPAB-hydrosilation. If hydrosilation is successful, a bond is created between the surface silicon and the terminal carbon of the MPAB. This bond is represented by the $\text{CSi}^*-(\text{OSi}\equiv)_3$ and $\text{CSi}^*-(\text{OH})(\text{OSi}\equiv)_2$ peaks at 66 and 54 ppm [3] respectively. The small percentage of MPAB found on the surface as compared to the silicon-hydroxide and -hydride groups, together with the limited mobility of surface silicons, may inhibit the detection of the Si-C resonance. Therefore, CP-MAS ^{29}Si NMR cannot confirm the success of hydrosilation.

4. CP-MAS ^{13}C NMR Spectra

The MPAB's CP-MAS ^{13}C NMR spectrum (Figure 9) was compared with that of the MPAB-bonded silica (Figure 10). MPAB's features were easily identified on the bonded silica. The signal of the Si-C bond is readily identified at 10.1 ppm [3,16]. This implies

that MPAB was chemically bonded to the silica surface (as the terminal carbon is in a more proton-surrounding and mobile environment than the surface silicon, Si-C resonance

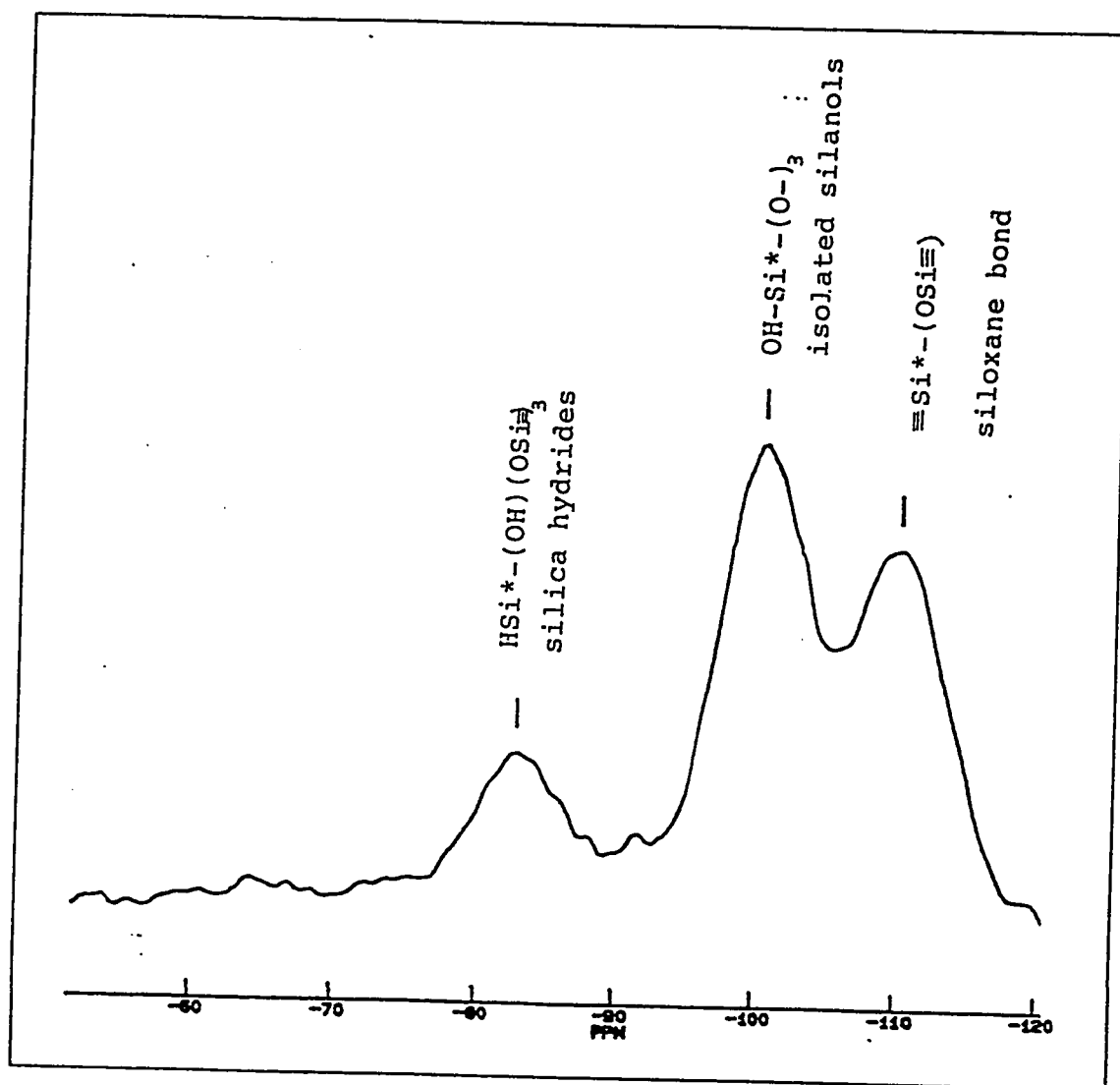


Figure 8. The CP-MAS ^{29}Si NMR Spectrum of MPAB-Bonded Silica

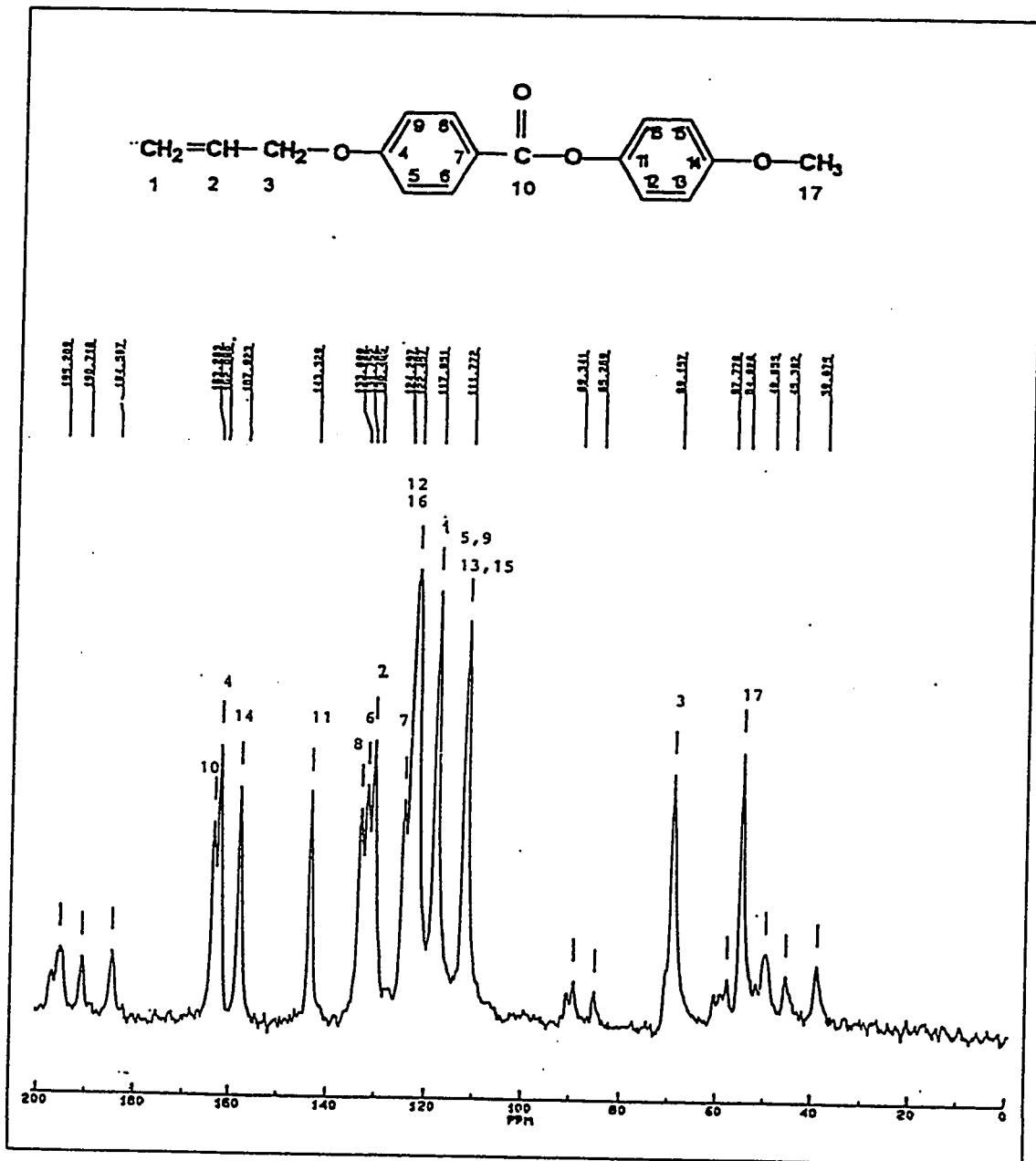


Figure 9. The CP-MAS ^{13}C NMR Spectrum of MPAB

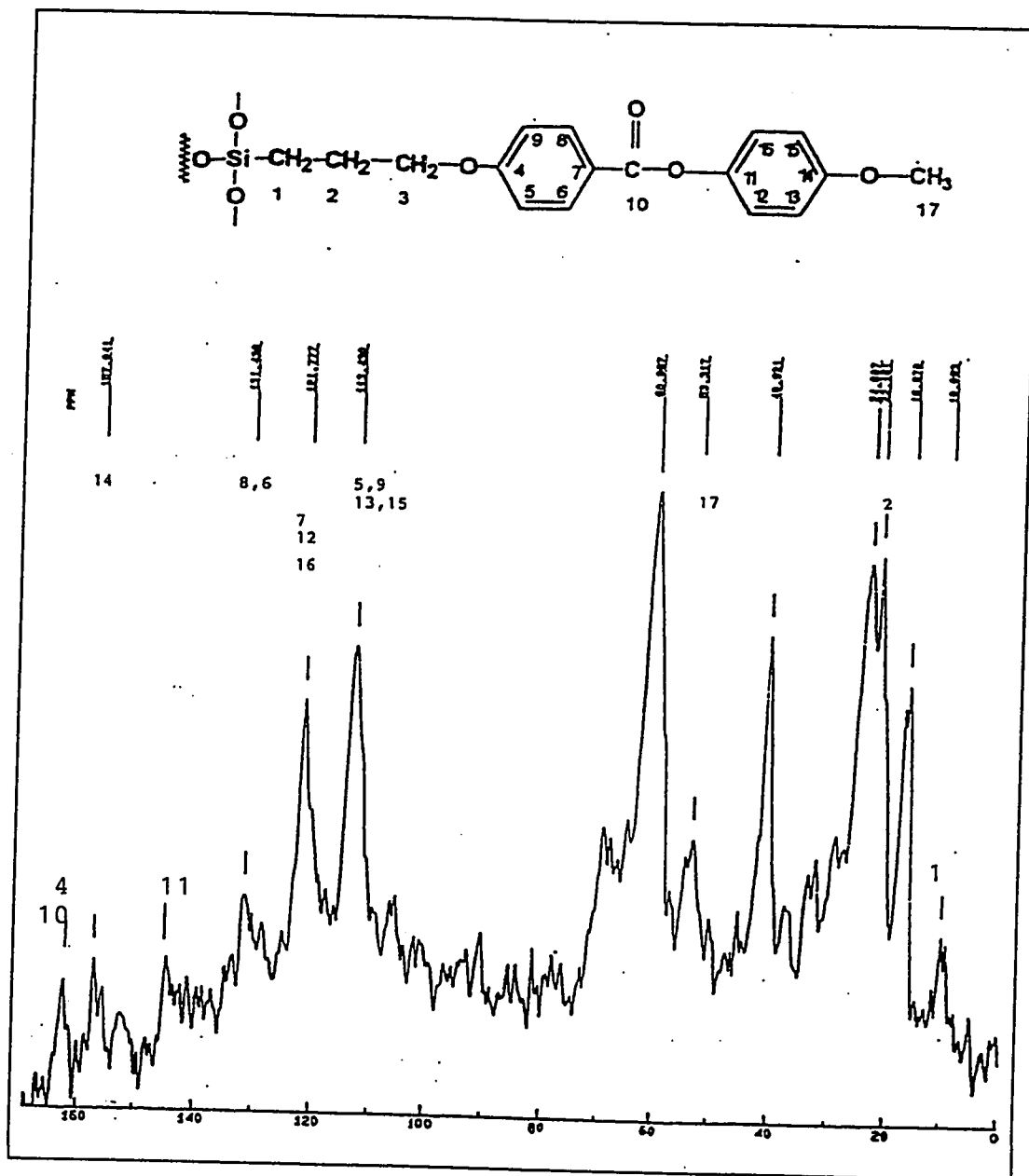


Figure 10. The CP-MAS ^{13}C NMR Spectrum of MPAB-Bonded Silica

silicon, Si-C resonance is observed in Figure 10). The peak at 24.0 ppm may indicate the silicon-addition to carbon 2, instead of to carbon 1 [16]. But due to the great steric hindrance and rigid structure of solid silica, silicon-C2 bond is not commonly observed. The 16.6 and 61.0 ppm peaks are caused by surface-adsorbed organic solvents, such as ethanol, on the silica surface. The source for the 40.8 ppm peak was uncertain. In spite of this, the CP-MAS ^{13}C NMR confirms that hydrosilation certainly occurred.

5. Carbon Analyses

Carbon analysis determines the quantity of MPAB bonded on the silica surface. After hydrosilation, the average percent carbon increased from 0.87 to 4.28. This large increase in carbon content must be due to the carbons on the skeleton of the bonded MPAB. To further confirm the hypothesis, a portion of an MPAB-bonded silica was rewashed according to the procedures on page 18 to eliminate any physically adsorbed MPAB. The average surface coverage before and after rewashing was 1.37 and $1.33 \mu\text{mol}/\text{m}^2$ respectively. Only a 3.6% change in surface coverage after rewashing verifies that virtually all of the MPAB was chemically bonded to the silica surface.

B . Reaction Variables Versus Surface Coverage Of MPAB-Bonded Phase

In reverse-phase chromatography, usually a higher surface coverage leads to better selectivity (see page 4). Therefore, the reaction variables (1) organic bonding material, (2) solvent for chloroplatinic acid hexahydrate, (3) catalyst : MPAB molar ratio, (4)

temperature, (5) reaction time, and (6) solvent (toluene) volume were varied one at a time to establish a condition that produced the highest surface-coverage bonded silica. This condition was repeated six times to determine the reproducibility of the MPAB-hydrosilation reaction. The standard deviation serves as the error bar for Figures 13 to 15 (see page 43 for results).

1. Organic Bonding Material

MPAB and cholesteryl-10-undecenoate (Figure 11) were first bonded to silica by

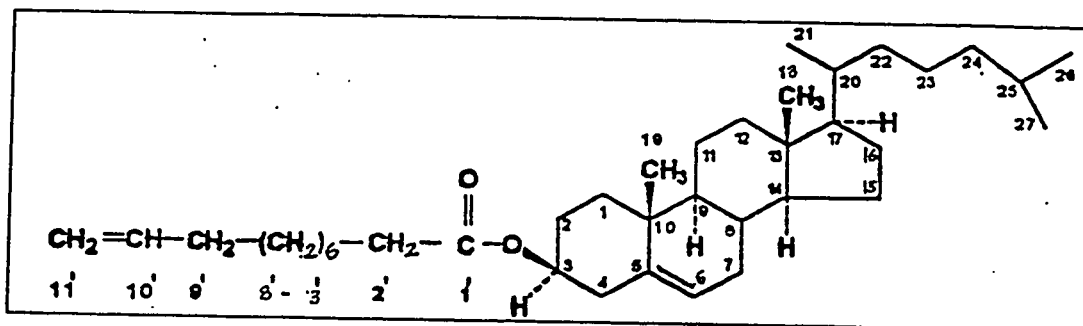


Figure 11. The Structure of Cholesteryl-10-Undecenoate

Speier's catalyst. As cholesteryl-10-undecenoate is bulkier than MPAB, the surface coverage of the former is expected to be less. The yields are tabulated in Table 3. Since samples were drawn twice during the 48-hour-hydrosilation of cholesteryl-10-undecenoate, some doubts arise as to the consistency of the solution matrices between the

samples and the remaining solution in the flask. Before further experiments were carried out to investigate how the organic bonding material affects surface coverage, a parallel study determined that higher yield was achieved with rhodium catalyzing the hydrosilation of cholesteryl-10-undecenoate. As a result, this research was focused on the optimization of the MPAB-hydrosilation. With only two sets of data, the structural effect of hydrocarbons on surface coverage cannot be determined.

Table 3 - The Surface Coverages of MPAB- and Cholesteryl-10-Undecenoate-Hydrosilations

| Bonded Material | Reaction Conditions | | Average Surface Coverage ($\mu\text{mol}/\text{m}^2$) |
|----------------------------|---------------------|---------------------------|---|
| | Reaction Time | Temperature | |
| MPAB | 48 hours | $100 \pm 2^\circ\text{C}$ | 0.77 |
| Cholesteryl-10-undecenoate | 48 hours | $100 \pm 2^\circ\text{C}$ | 0.46* |
| MPAB | 96 hours | $100 \pm 2^\circ\text{C}$ | 0.52 |
| Cholesteryl-10-undecenoate | 96 hours | $100 \pm 2^\circ\text{C}$ | 0.50 |

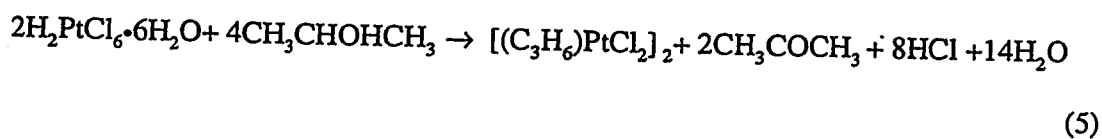
NOTE : * After 100°C was reached, approximately 2 ml of sample was withdrawn from the reaction flask at the second and the twenty-fourth hours.

2. Solvent For Chloroplatinic Acid Hexahydrate

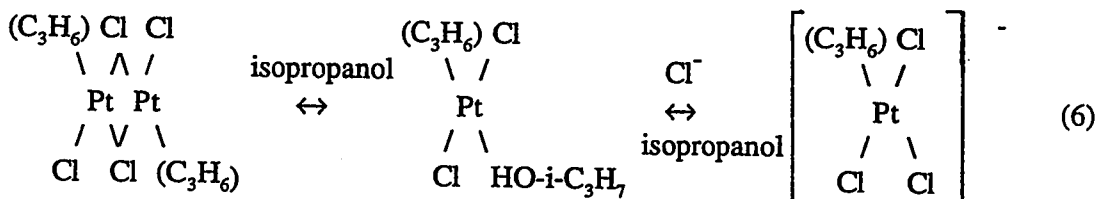
The hydrosilation reaction developed by Speier *et al.* [1] (see page 1) was catalyzed by chloroplatinic acid hexahydrate dissolved in isopropanol ((CH₃)₂CHOH). When the catalyst : MPAB molar ratio was increased from 2 X 10⁻⁵ to 1 X 10⁻³, the surface coverage was increased from 0.7 to 1.5 μmol/m². The change in molar ratio was accomplished by adding 980 μl, instead of 22.8 μl of the 8 X 10⁻⁴ M Speier's catalyst solution. But with 980 μl of the catalyst solution, an azeotrope of isopropanol and toluene was formed at 92 °C because isopropanol contributed to one-seventh of the total solvent volume.

Occasionally, if isopropanol was trapped by capillary action between the thermometer and the wall of the flask, the reaction mixture could reach 100°C. Yet this situation was not always reproducible. Hence, isopropanol was replaced by isopentanol ((CH₃)₂CHCH₂CH₂OH) which boils at 128.5 °C. Thereafter, no further temperature fluctuation problems were encountered.

Chalk and Harrod [17] proposed a scheme for Speier's catalyst in the homogenous hydrosilation reaction. More information was added later by Benkeser and Kang [18]. This model was modified by Sandoval and Pesek [3] to explain the heterogeneous reaction using Speier's catalyst. In order to catalyze hydrosilation, chloroplatinic acid hexahydrate is first reduced by isopropanol to platinum(II) as in equation 5 [18].



The propyleneplatinum dimer further restructures in the presence of chloride ions, according to equation 6 [18].



During the induction period, the incoming olefin (MPAB in this case) exchanges with the propylene group on the platinum complex to form the catalyzing complex ([olefin•PtCl₃]⁻) for hydrosilation [18].

When platinum is reduced, isopropanol is oxidized to acetone. Therefore, if isopentanol shares the same catalytic mechanism as isopropanol, 3-methylbutanal will be produced. Benkeser and Kang [18] evaporated the solvent of Speier's catalyst in vacuum, and analyzed both the distillate and the residue by infrared spectroscopy. The spectrum of the distillate shows a feature at 1715 cm⁻¹ which corresponds to the carbonyl stretching of acetone. The C-H stretch of the coordinated olefin occurs between 3100 to 3000 cm⁻¹ [19]. A similar study was carried out on the chloroplatinic acid hexahydrate-isopentanol solution. An attempt was made first to separate the solvent and the residue of the catalyst solution by vacuum distillation at room temperature. However, no distillate was collected. Finally, the entire catalyst solution was analyzed (Figure 12). Strong O-H (3200 to 3300 cm⁻¹) and C-O (1070 cm⁻¹) stretchings of alcohol are found. But no carbonyl stretching signal (about 1720 cm⁻¹) is observed to support the production of 3-methylbutanal. No olefinic C-H stretch signal (3100 to 3000 cm⁻¹) was detected for the [MPAB•PtCl₃]⁻

pentylene. Possibly only a small amount of the $[\text{C}_5\text{H}_{10}\cdot\text{PtCl}_3]^-$ complex was present. Hence, its functional-group resonances were obstructed by that of the abundant isopentanol.

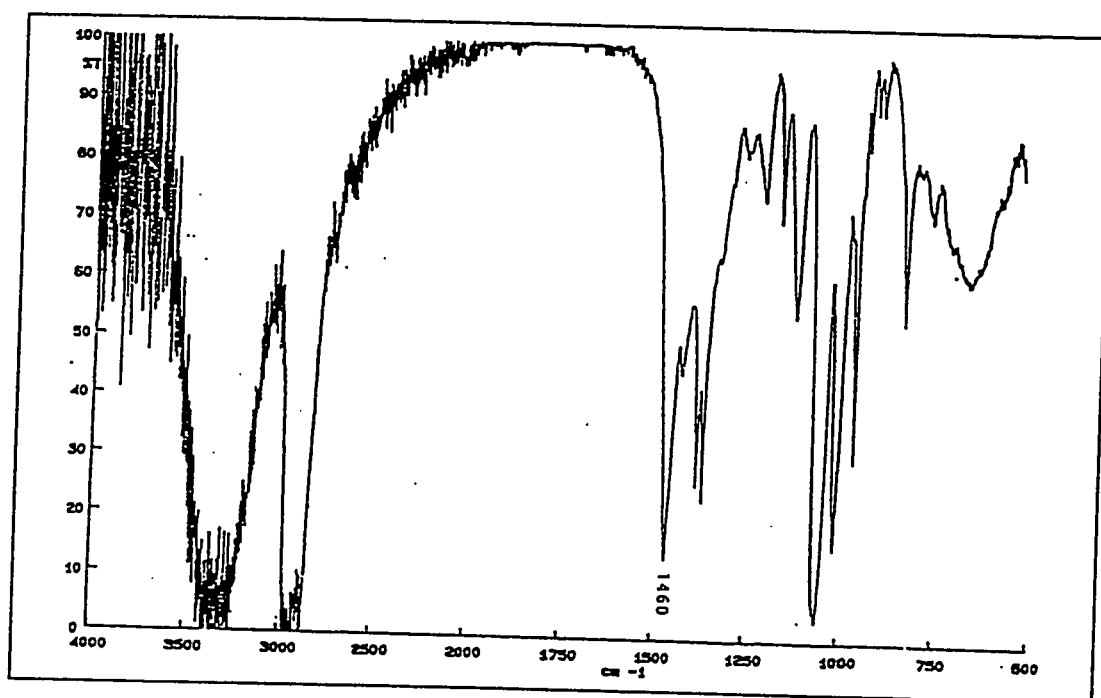


Figure 12. The FTIR Spectrum of Chloroplatinic Acid Hexahydrate in Isopentanol

Alternatively, MPAB may reduce platinum(IV) to form the catalyzing species, $[\text{MPAB}\cdot\text{PtCl}_3]^-$, during the induction period. However, no evidence was collected to verify this theory. The third possibility is that platinum(IV) catalyzed hydrosilation without altering its oxidation state. This means that the chloride ligands on the

platinum(IV) complex are substituted with MPAB, silicon and hydrogen. However, according to Hartley [20], any ligand-substitution reaction of platinum(IV) is catalyzed by platinum(II). Therefore, an oxidation-reduction reaction must take place on chloroplatinic acid hexahydrate to produce the catalyzing species because no platinum(II) was available. Future studies should investigate the formation of $[\text{MPAB}\cdot\text{PtCl}_3]^-$ complex and the catalytic mechanism involving isopentanol. But most importantly, the CP-MAS ^{13}C NMR spectrum of the MPAB-bonded silica proves that successful hydrosilation took place.

3. Catalyst : MPAB Molar Ratio

Catalyst : MPAB molar ratios of 2×10^{-1} , 2×10^{-2} , 2×10^{-3} , 1×10^{-3} and 1×10^{-5} were investigated while other variables were held constant. The results are plotted in Figure 13. The optimum ratio is between 2×10^{-3} to 1×10^{-3} . At the two extremes, the surface coverages were lower because at the 1×10^{-5} molar ratio the amount of catalyzing species ($[\text{MPAB}\cdot\text{PtCl}_3]^-$) was limited. At the molar ratio of 2×10^{-1} , part of the catalyzing species was converted to the black zero-valent platinum. Therefore, the amount of $[\text{MPAB}\cdot\text{PtCl}_3]^-$ available for hydrosilation was limited. In fact, a grayish color was

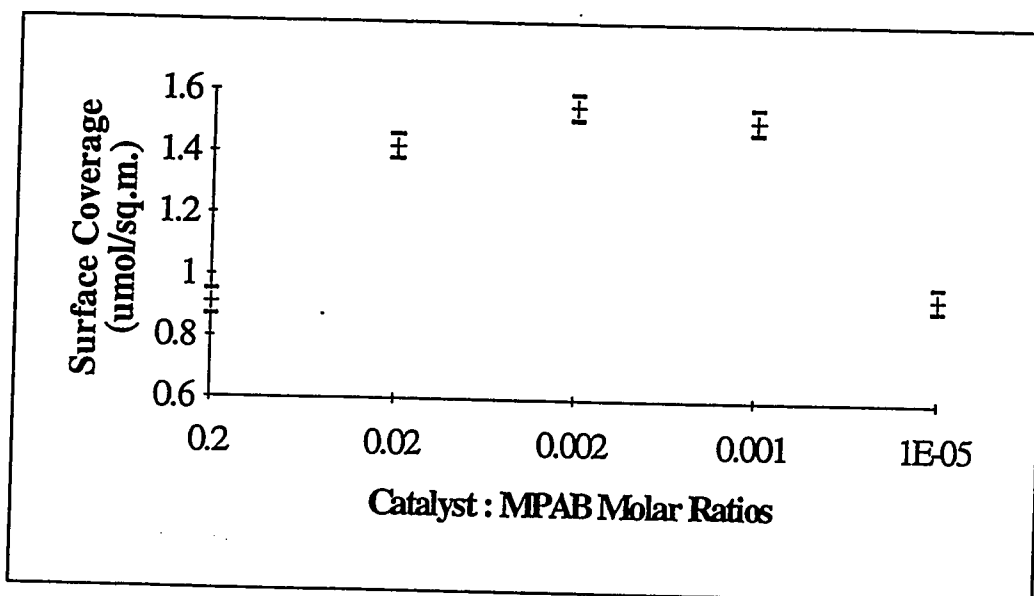
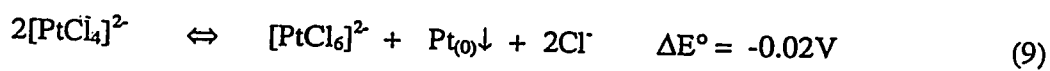
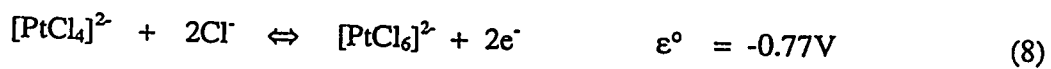
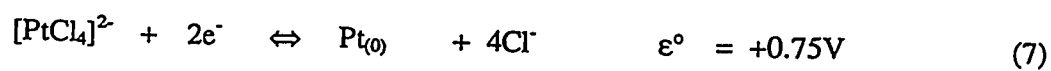


Figure 13. Plot of Catalyst : MPAB Molar Ratios versus Surface Coverage

observed on MPAB-bonded silica at 2×10^{-1} and 2×10^{-2} molar ratios. Sandoval and Pesek [3] also observed a similar phenomena at high temperatures and long reaction times when they bonded C18 to a silica-hydride surface. The oxidation-reduction of platinum occurs in the following fashion [20]:



$$\Delta G^\circ = -n\mathfrak{F}\Delta E^\circ \quad (10)$$

In equation 10, ΔG° is the Gibbs free energy change, n refers to the moles of electrons transferred in equation 7 and 8, \mathfrak{F} represents the Faraday constant ($9.65 \times 10^4 \text{ C/mol}$), ε°

indicates the standard potential of the half-cell reaction and ΔE° is the change in standard potentials in the net equation 9.

A rather small ΔG° (3.86 kJ/mol) is calculated from equation 10. Since $[\text{MPAB}\cdot\text{PtCl}_3]^-$ is structurally quite similar $[\text{PtCl}_4]^{2-}$, the ΔG° of the reaction of $[\text{MPAB}\cdot\text{PtCl}_3]^-$ should be comparable. This means that under most conditions, the formation of $[\text{MPAB}\cdot\text{PtCl}_3]^-$ is favored; no grayish product is observed. On the other hand, at high catalyst concentrations or high temperatures [3], by the LeChatelier's Principle, the black solid platinum(0) is favored producing a grayish MPAB-bonded silica. Consequently, the availability of $[\text{MPAB}\cdot\text{PtCl}_3]^-$ for hydrosilation diminishes. The surface coverage in these situations is lower.

4 . Temperature

The effect of temperature on hydrosilation (Figure 14) was studied between 70 to 108 °C. Temperatures lower than 70 °C were not feasible because a minimum energy is required to form the $[\text{MPAB}\cdot\text{PtCl}_3]^-$ complex. The upper limit was set by the boiling point of toluene at about 110 °C. Because the carbon percent of the silica hydride for synthesizing these four MPAB-bonded silica was not determined, the surface coverages of the bonded silicas could not be calculated. Instead, the carbon percent of the MPAB-bonded silicas (P_c) (see page 12 for explanation) were compared.

The transition-state theory explains how temperature affects a reaction. First, enough energy has to be supplied to the reactants to initiate collision. During collision, the reactants form an activation complex when the reactant molecules are properly orientated. The collision energy is then transferred to the bonds of the complex. At higher temperatures, more collisions take place. The chance of forming the activation complex increases. Occasionally, all collision energy is concentrated in one bond. The activation complex will then dissociate to form the products if equal or greater than the activation energy is contained in the activation complex. Otherwise, the complex will dissociate to regenerate the reactants [21].

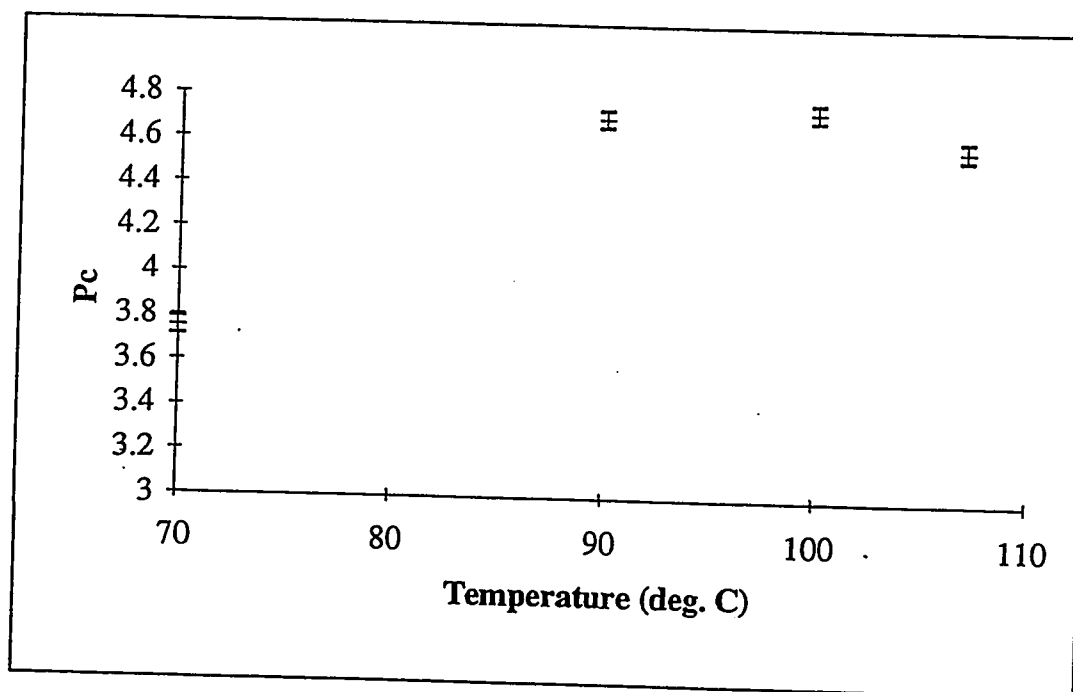


Figure 14. Plot of Temperature versus P_c.

At a temperature of 70 °C in the MPAB-hydrosilation, the surface coverage was low because not many reactant molecules possessed enough activation energy to overcome the energy barrier. At the upper temperature limit of 108 °C, some undetermined factors may activate the cleavage of the bonded MPAB from the silica surface or decompose the activation complex. The surface coverage was maximized only between 90 to 100 °C. To ensure most reactants had adequate energy for hydrosilation, 100 °C was chosen as the reaction temperature.

5 . Reaction Time

As solid silica is porous, time is required for the reactants to diffuse into the pores, especially for the narrower ones, before the reaction with the surface hydrides. Therefore, the surface coverages attained with various reaction time are dependent upon the surface properties of silica. For the Vydac 101TP silica, the relationship between surface coverage and reaction time is shown in Figure 15. Most of the hydride sites were reacted between 48 to 120 hours of reaction time. After 120 hours, hydrosilation may take place further on the hydrides in the narrower pores. Since most of the reaction occurred after 48 hours, this was chosen as the optimum reaction time.

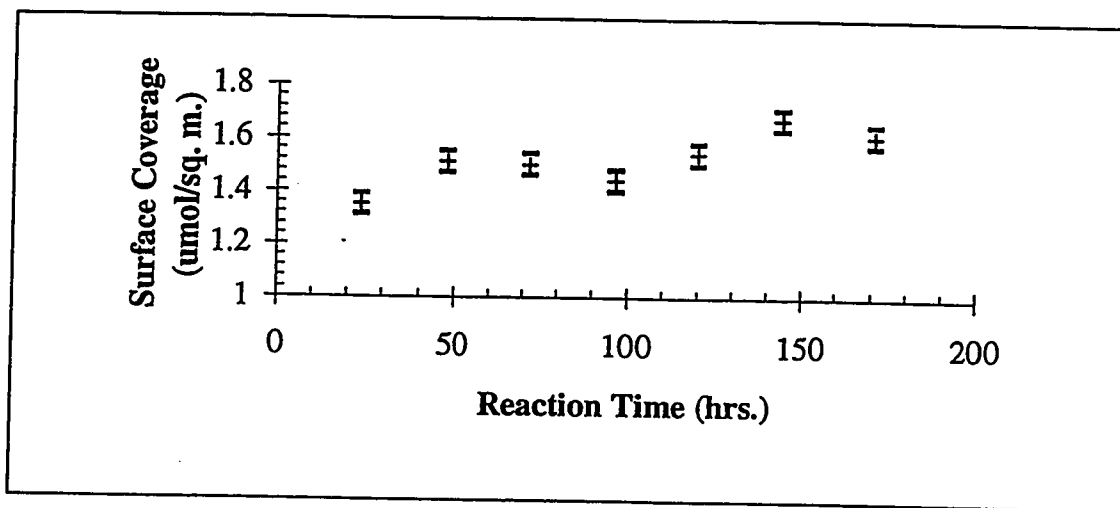


Figure 15. Plot of Reaction Time versus Surface Coverage

6. Solvent (Toluene) Volume

Often a higher concentration of reactants results in a higher yield. When the solvent volume was decreased from 6.2 to 3.1 ml, the surface coverage increased to 1.77 from 1.51 $\mu\text{mol}/\text{m}^2$ on average as predicted. However, when the 3.1-ml reactant matrix was scaled up by three fold to produce enough bonded silica for column packing, the surface coverage dropped to 0.96 $\mu\text{mol}/\text{m}^2$. The product also appeared grayish. As discussed on page 39, the grayish color reflects a loss of the catalytic activity at the extreme concentrations. A low surface-coverage bonded silica is resulted. Therefore, the optimum toluene volume was 6.2 ml.

After determining the optimum condition for each reaction variable, the MPAB-hydrosilation was repeated six times under these conditions (see page 17 for procedures). The average surface coverage was $1.51 \mu\text{mol}/\text{m}^2$ with a standard deviation of 0.04 and a spread of $0.10 \mu\text{mol}/\text{m}^2$.

C . Chromatographic Studies

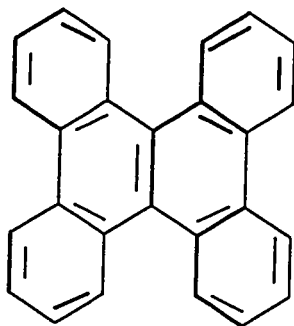
Three MPAB-bonded silicas with surface coverages of 0.97, 1.41 (grayish) and 1.66 (grayish) $\mu\text{mol}/\text{m}^2$ were packed into columns labeled 1, 2 and 3 respectively. These MPAB stationary phases were first compared with the conventional C18 stationary phases for the separation of a PAH mixture (SRM 869). Then the selectivities of an isomeric PAH-mixture (SRM 1647c) on the MPAB stationary phases were studied. Lastly, the efficiency of column 3 was determined, and a retention mechanisms of the MPAB and the C18 stationary phases were compared.

1 . Separations Of SRM 869

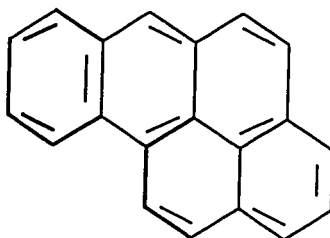
The selectivities of structural isomers on a monomeric, an oligomeric (an intermediate of monomeric and polymeric) and a polymeric C18 stationary phases [8, 22] are different. Because the polymeric phase is the most hydrophobic and the C18 ligands interact the most with their neighbors, a rigid intermolecular space is created to selectively retain planar analytes longer [8]. Due to these reasons, the elution order of the analytes of the

SRM 869 mixture (Figure 16) varies with the C18 phase type (Figure 17) [9]. As a result, using the same separation conditions on the MPAB columns, MPAB-MPAB interactions can be correlated with the C18 model. Since the concentrations of the three solutes of the SRM 869 differ, the elution order of the mixture can be identified by the peak height of individual solute.

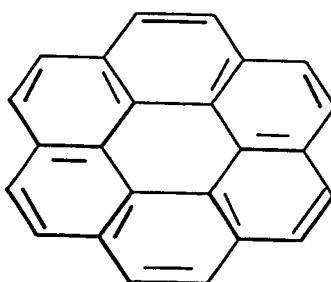
The mixture coeluted at 1.09 min on column 1 (Figure 18). Because of insufficient data, the phase type for this bonded material was not determined. The separation (Figure 19) on column 2 resembles that of the oligomeric C18 phase. Finally, for column 3, due to high back pressure, the flowrate was decreased to one ml/min. Although a slower flowrate prolongs the retention time of all analytes, the elution order is not affected. Detection at 210 and 254 nm was employed for column 3 because potassium nitrate, which has a stronger absorption at 210 nm, was injected with the SRM 869 mixture. As observed in Figure 20, BaP coeluted with TBN, suggesting an oligomeric-polymeric C18 like intermolecular space configuration. Therefore, increasing the surface coverage of MPAB on silica enhances the MPAB-MPAB interaction on the stationary phase.



1,2:3,4:5,6:7,8-tetrabenzonaphthalene (TBN)



Benzo[*a*]pyrene (BaP)



Phenanthro[3,4-*c*]phenanthrene (PhPh)

Figure 16. The Structures of the Components in SRM 869

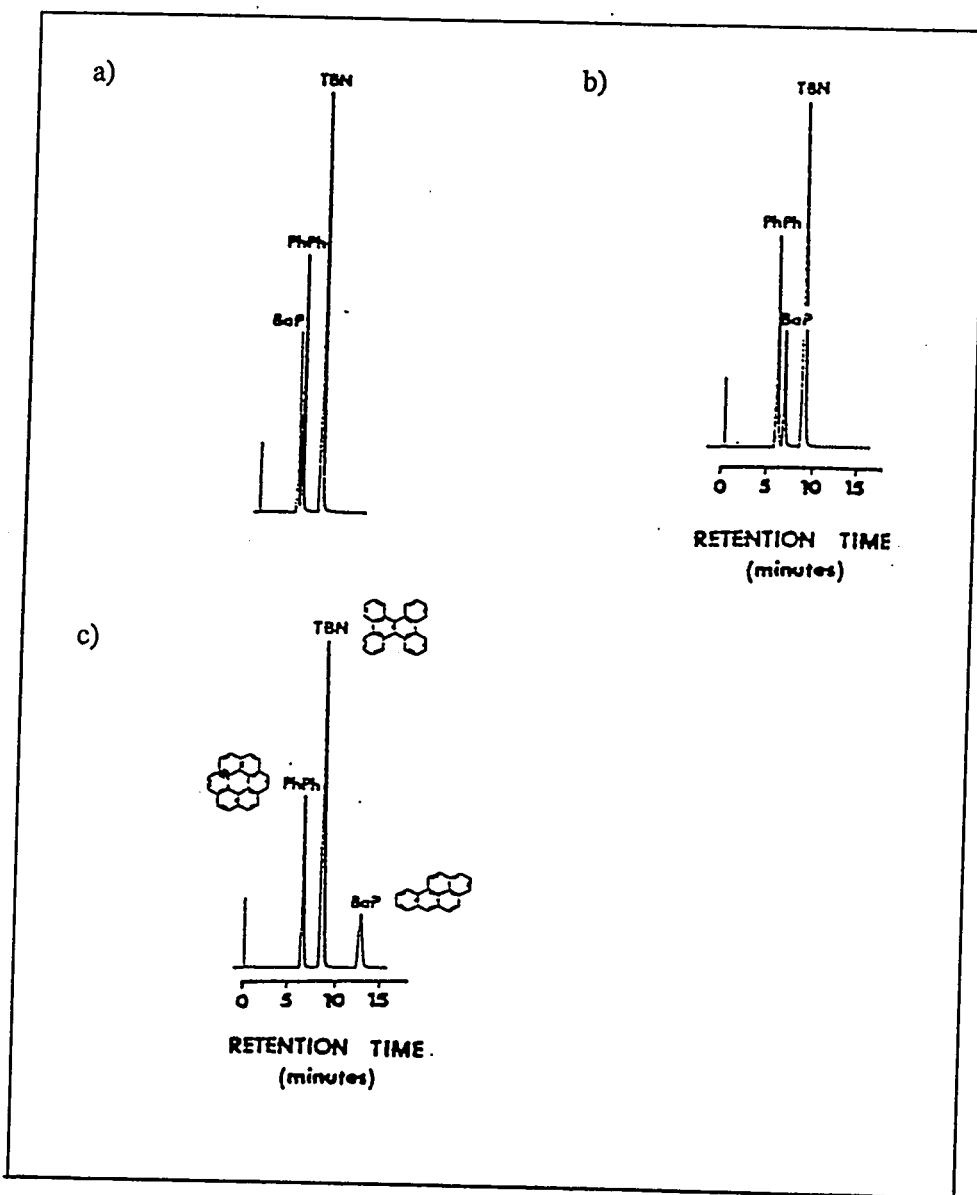


Figure 17. The Chromatograms of SRM 869 on (a) Monomeric-C18, (b) Oligomeric-C18 and (c) Polymeric-C18 Phases

(Flowrate of 2 ml/min.; mobile phase of 85:15 ACN/water; temperature of 25°C)

Reprinted with permission from Sanders, L.C.; Wise, S.A. *Anal. Chem.* 1984, 56, 504-510 (Copyright 1984 American Chemical Society).

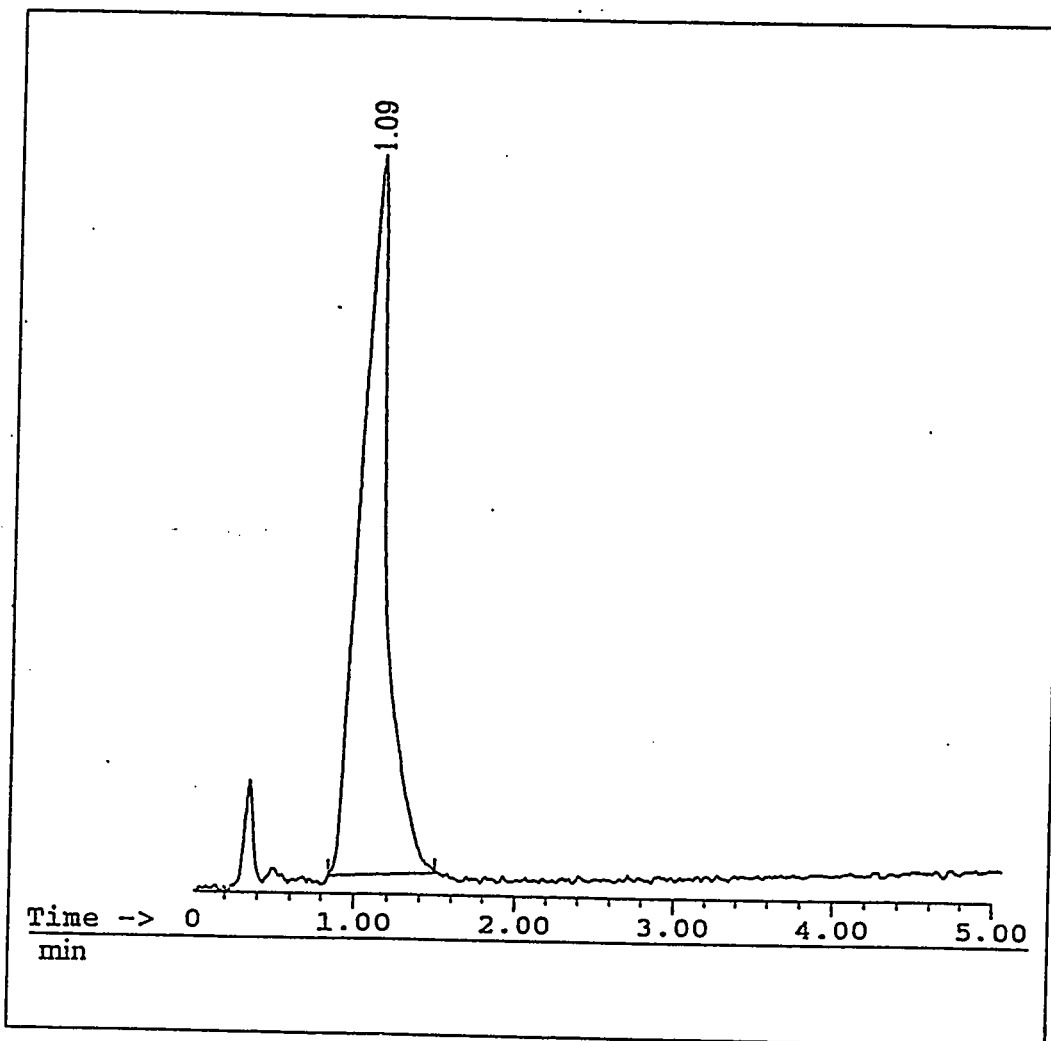


Figure 18. The Chromatogram of SRM 869 on Column 1 with 85:15 ACN/Water (Flowrate of 2 ml/min.; detection at 254 nm)

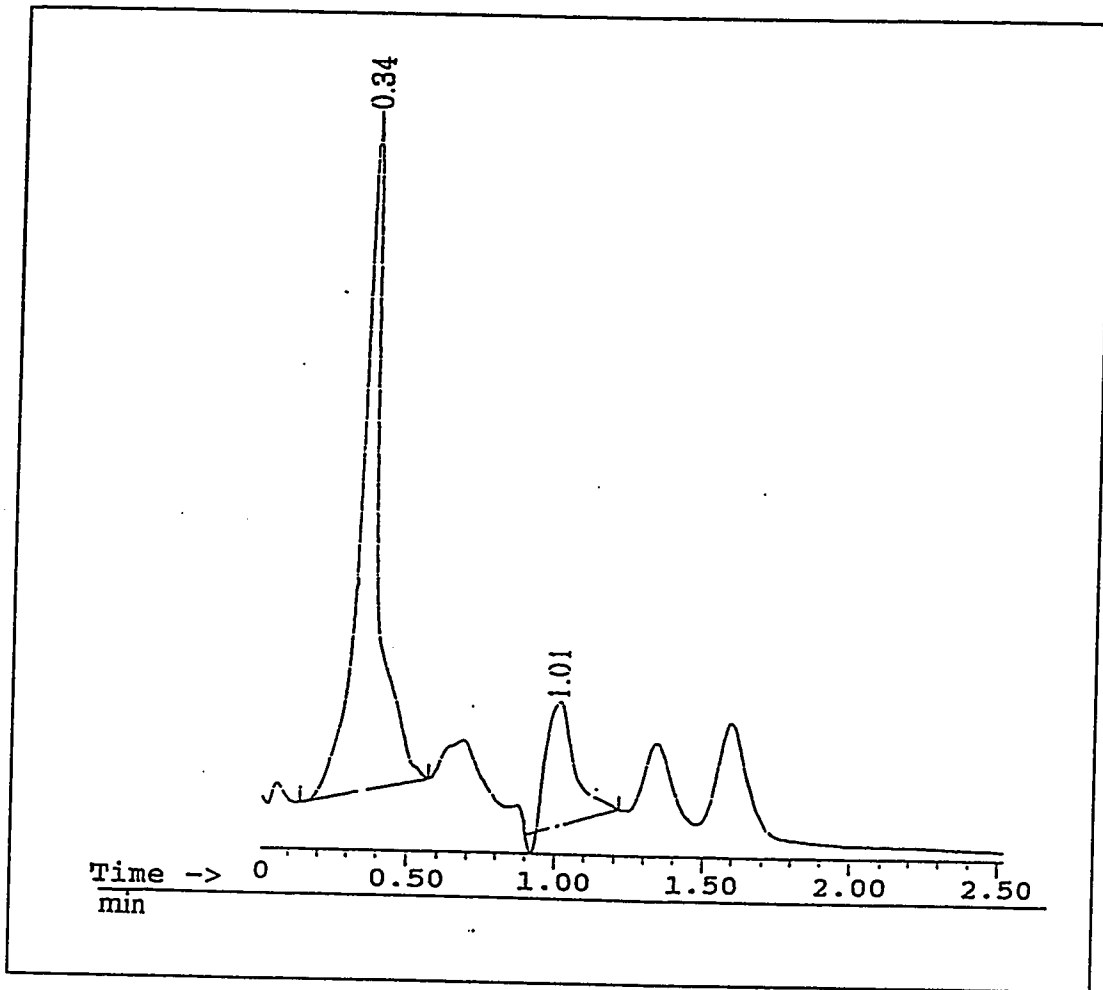


Figure 19. The Chromatogram of SRM 869 on Column 2 with 85:15 ACN/water (Flowrate of 2 ml/min.; detection at 254 nm)

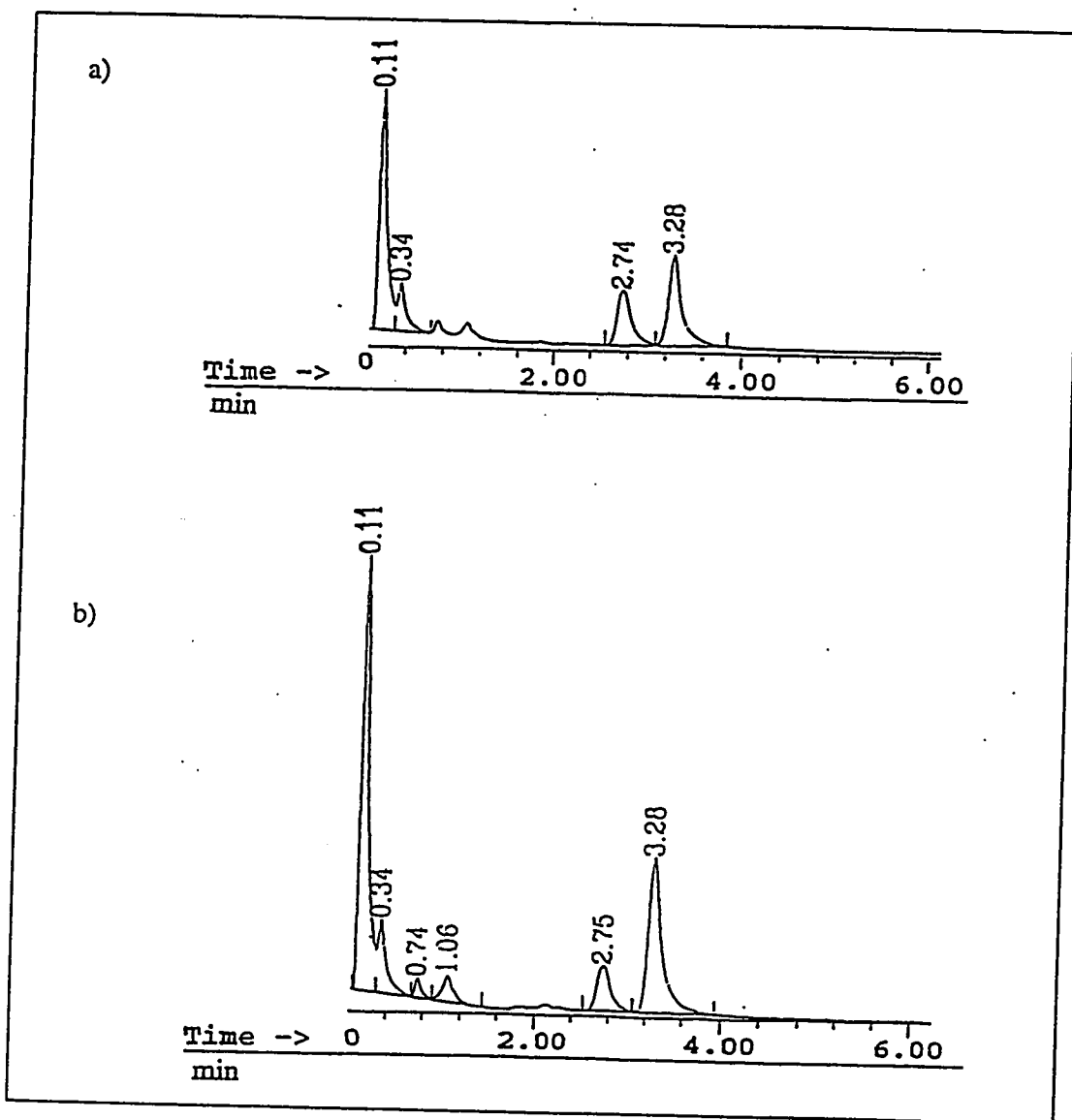


Figure 20. The Chromatograms of SRM 869 on Column 3 with 85:15 ACN/water (a) at 254 and (b) 210 nm (Flowrate of 1 ml/min.)

2 . Separations Of SRM 1647c

Out of the 16 PAHs, SRM 1647c (Figure 21) contains five sets of structural isomers. The formula weights and the length-to-breath ratio (L/B) of all 16 PAHs are tabulated in Table 4. The L/B ratio measures the maximum length and breath of a rectangle that encloses the entire molecule in two-dimensions [8, 23]. Hence, a higher L/B value refers to a "longer" analyte.

a . Isocratic Separations

Separations of SRM 1647c were carried out isocratically with methanol and acetonitrile as the modifier, and in gradient conditions using methanol-, ACN- and THF-water mixtures. The best separations for each isocratic condition on column 1 and 2 are shown in Figure 22 and Figure 23. When methanol acted as the organic modifier, more separation occurred on both column 1 and 2. Due to the high back pressure, column 3 was not tested. The more polar methanol drives analytes to partition more with the MPAB stationary phase. Higher selectivity and longer retention times are observed. Furthermore, in order to achieve the same degree of separation between columns of different surface coverages, a lower water-content mobile phase was employed for column 2 (higher surface coverage). This indicates that with more MPAB bonded to the silica surface, the hydrophobicity of the stationary phase increases. Hence, a less polar mobile phase enables effective analyte-stationary phase interaction.

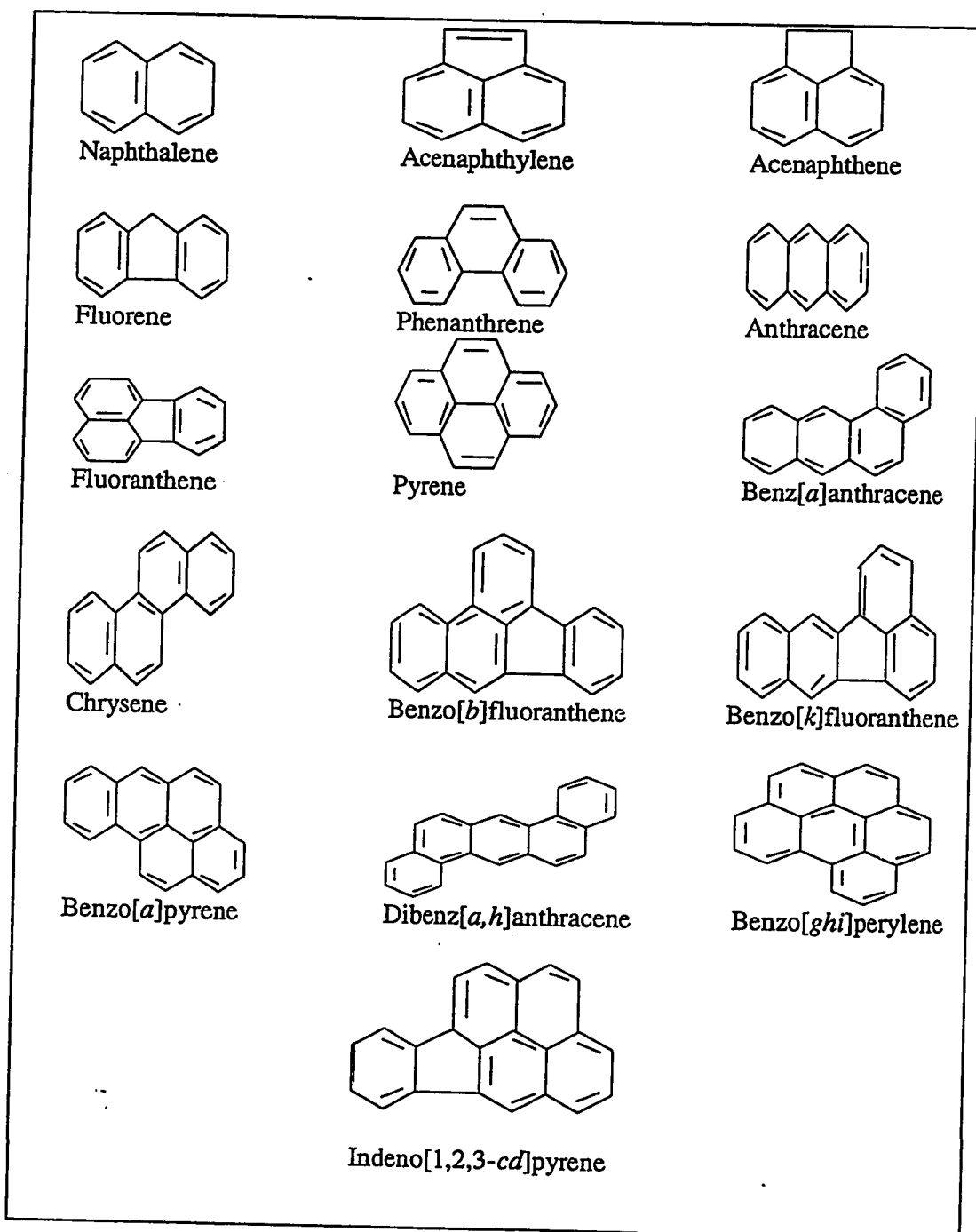


Figure 21. The Structures of the Components of SRM 1647c

Table 4 - The Formula Weights and the L/B Ratios of the SRM 1647c Analytes

| Solutes (g/mol) | L/B Ratio | Formula Weight |
|------------------------|------------------|-----------------------|
| Naphthalene | 1.24 | 128.19 |
| Acenaphthylene | 1.08 | 152.21 |
| Acenaphthene | 1.06 | 154.21 |
| Fluorene | 1.57 | 166.23 |
| Phenanthrene | 1.46 | 178.24 |
| Anthracene | 1.57 | 178.24 |
| Fluoranthene | 1.22 | 202.76 |
| Pyrene | 1.27 | 202.76 |
| Benz[a]anthracene | 1.58 | 228.30 |
| Chrysene | 1.72 | 228.30 |
| Benzo[k]fluoranthene | 1.48 | 252.32 |
| Benzo[a]pyrene | 1.50 | 252.32 |
| Benzo[b]fluoranthene | 1.78 | 252.32 |
| Indeno[1,2,3-cd]pyrene | 1.40 | 276.34 |
| Benzo[ghi]perylene | 1.12 | 276.34 |
| Dibenz[a,h]anthracene | 1.79 | 278.36 |

Reprinted from Sanders, L.C.; Wise, S.A. *Advances in Chromatogr.* **1986**, *25*, 186-187 (by the courtesy of Marcel Dekker, Inc., NY).
 Jinno, K.; Kawasaki, K. *J. Chromatogr.* **1984**, *316*, 6 (Copied with permissions).

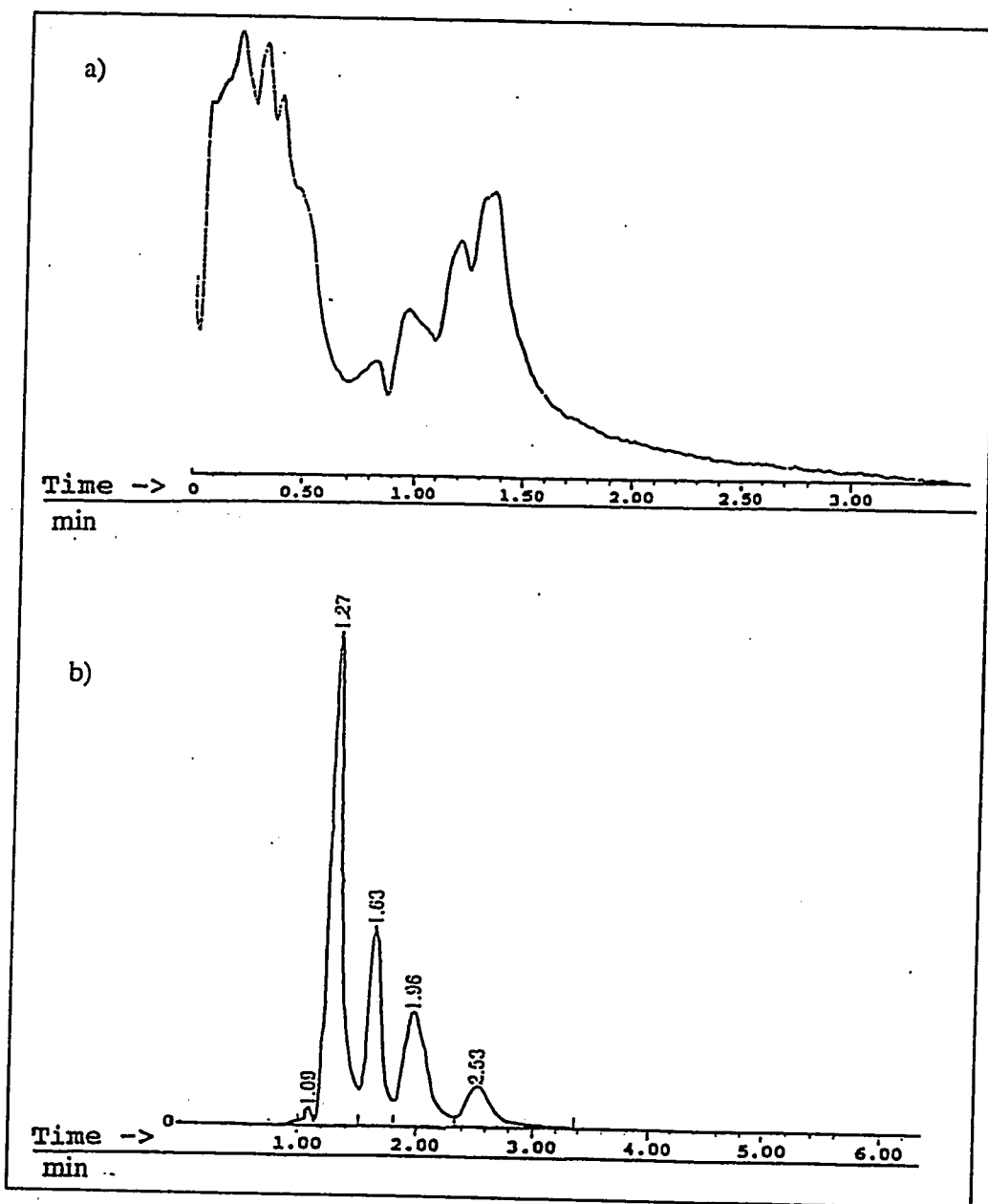


Figure 22. The Chromatograms of SRM 1647c on Column 1 with (a) 80:20 ACN/Water and (b) 50:50 Methanol/Water
(Flowrate at 2 ml/min.; detection at 254 nm)

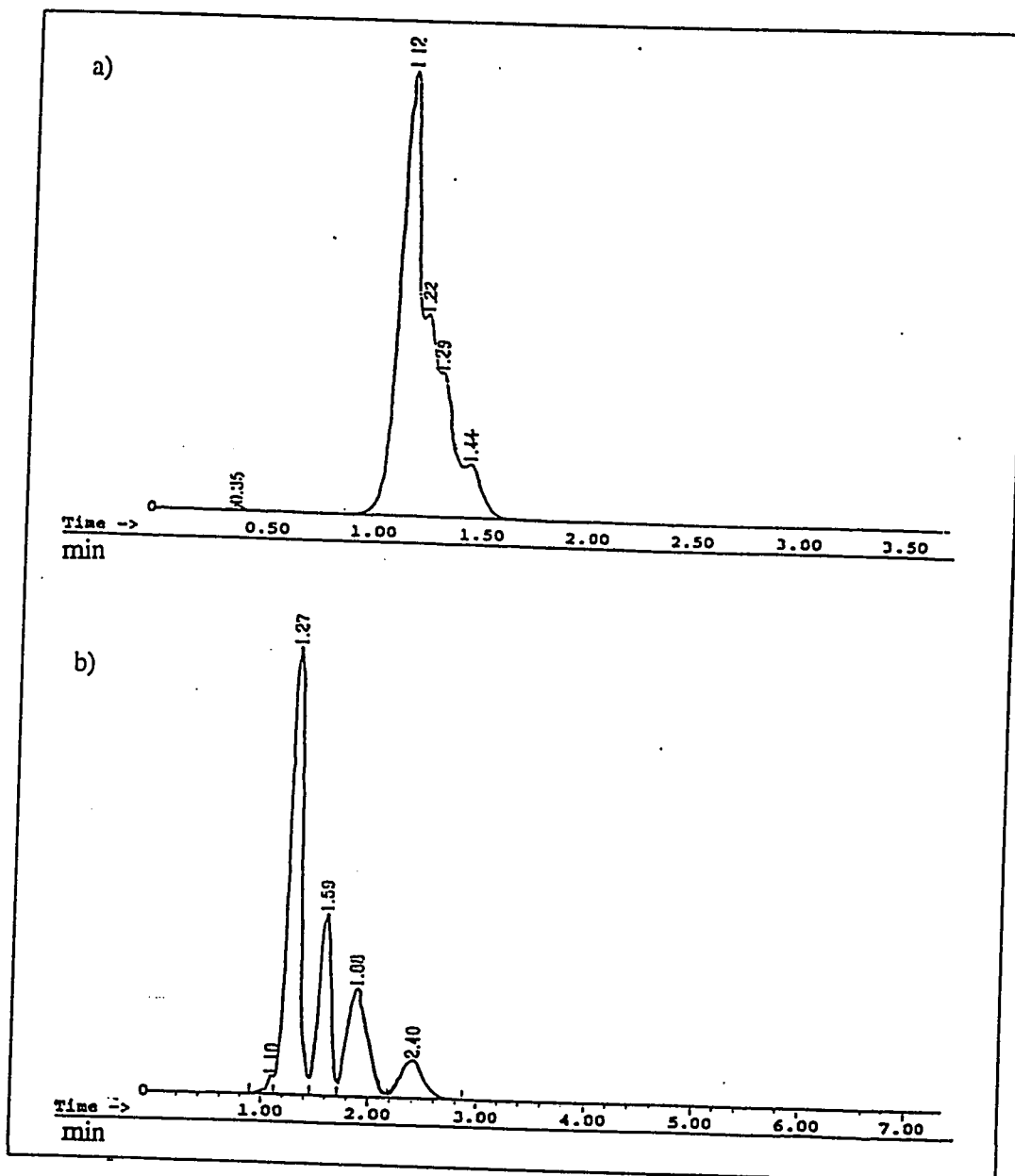


Figure 23. The Chromatograms of SRM 1647c on Column 2 with (a) 85:15 ACN/Water and (b) 80:20 Methanol/Water (Flowrate at 2 ml/min.; detection at 254 nm)

b . Gradient Separations

Gradient separations of the SRM 1647c mixture were performed on monomeric, oligomeric and polymeric C18 phases (Figure 24). Based on this condition, the gradients (Table 5) employed on the three MPAB columns were developed. High viscosity [24], resulting in enormous back pressure, precluded the use of methanol as the modifier for gradient separation on column 3. The physical properties of the THF/water mixture also created an intolerable back pressure for column 2. The flowrate was lowered to one ml/min for the separations. The chromatograms of gradient separations on the three columns are shown from Figure 25 to Figure 31. Since column 3 (Figure 27 and Figure 28) resolved the SRM 1647c into the greatest number of peaks and into the narrowest peaks, the retention times of several solutes were determined by resolving each analyte on column 3 under the same gradient condition. Naphthalene, fluorene, phenanthrene, anthracene, pyrene, chrysene and dibenz[*a,h*]anthracene were studied. The elution order of these seven solutes are the same on the MPAB and the C18 phases. This suggests that the retention mechanism of C18 phases may be comparable to that of the $1.66\mu\text{mol}/\text{m}^2$ -MPAB phase. By comparing to the SRM 1647c-separations on the C18 phases, the retention order of the other analytes on column 3 (Figure 27 and Figure 28) were deduced. Among the five structural isomeric pairs, only the retention times of phenanthrene and anthracene are absolutely certain because they were determined experimentally.

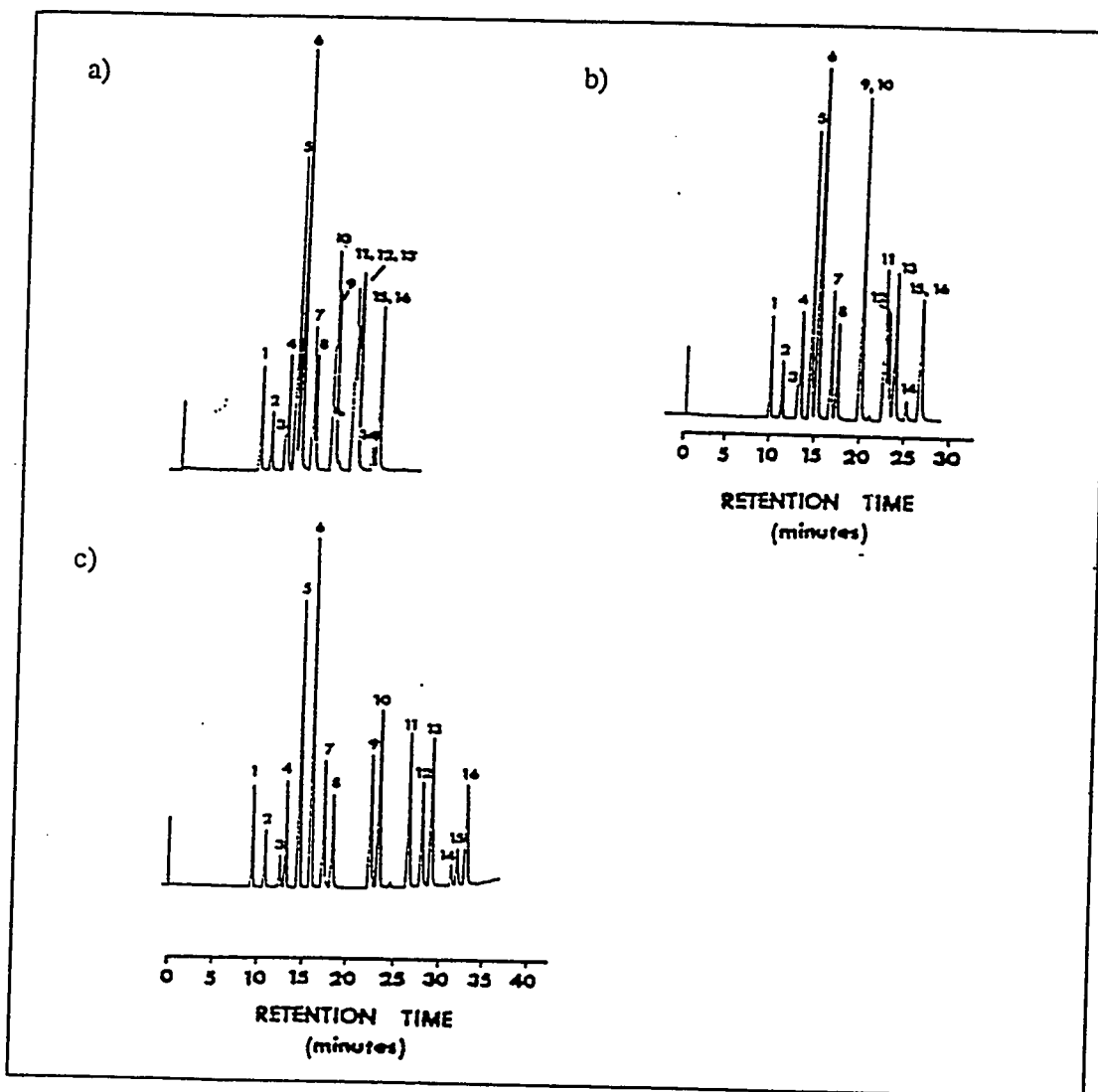


Figure 24. The Chromatograms of SRM 1647c on (a) Monomeric-C18, (b) Oligomeric-C18 and (c) Polymeric-C18 Phases

(40 to 100% acetonitrile in water over 30 min at 2 ml/min)

(1) Naphthalene, (2) Acenaphthylene, (3) Acenaphthene, (4) Fluorene, (5) Phenanthrene, (6) Anthracene, (7) Fluoranthene, (8) Pyrene, (9) Benz[*a*]anthracene, (10) Chrysene, (11) Benzo[*b*]fluoranthene, (12) Benzo[*k*]fluoranthene, (13) Benzo[*a*]pyrene, (14) Dibenz[*a,h*]anthracene, (15) Benzo[*ghi*]perylene, (16) Indeno[1,2,3-*cd*]pyrene

Reprinted with permission from Sanders, L.C.; Wise, S.A. *Anal. Chem.* 1984, 56, 504-510 (Copyright 1984 American Chemical Society).

Table 5 - Gradient Conditions Employed for the Study of SRM 1647c

- (i) flowrate = 2 ml/min.; three-minute hold at 50:50 ACN/water, then 15 minute linear gradient to 100% acetonitrile; 254 nm detection.
- (ii) flowrate = 2 ml/min.; two-minute hold at 35:65 ACN/water, then 16 minute linear gradient to 100% acetonitrile; 254 nm detection.
- (iii) flowrate = 1 ml/min.; four-minute hold at 35:65 ACN/water, then 32 minute linear gradient to 100% acetonitrile; 254 and 214 nm detection.
- (iv) flowrate = 1 ml/min.; four-minute hold at 50:50 ACN/water, then 32 minute linear gradient to 100% acetonitrile; 254 and 214 nm detection.
- (v) flowrate = 2 ml/min.; three-minute hold at 50:50 methanol/water, then 15 minute linear gradient to 100% acetonitrile; 254 nm detection.
- (vi) flowrate = 2 ml/min.; two-minute hold at 35:65 methanol/water, then 16 minute linear gradient to 100% acetonitrile; 254 nm detection.
- (vii) flowrate = 2 ml/min.; two-minute hold at 35:65 methanol/water, then 14 minute linear gradient to 100% acetonitrile; 254 nm detection.
- (viii) flowrate = 1 ml/min.; two-minute hold at 35:65 THF/water, then 14 minute linear gradient to 100% acetonitrile; 254 nm detection.
- (ix) flowrate = 1 ml/min.; three-minute hold at 50:50 THF/water, then 15 minute linear gradient to 100% acetonitrile; 254 nm detection.

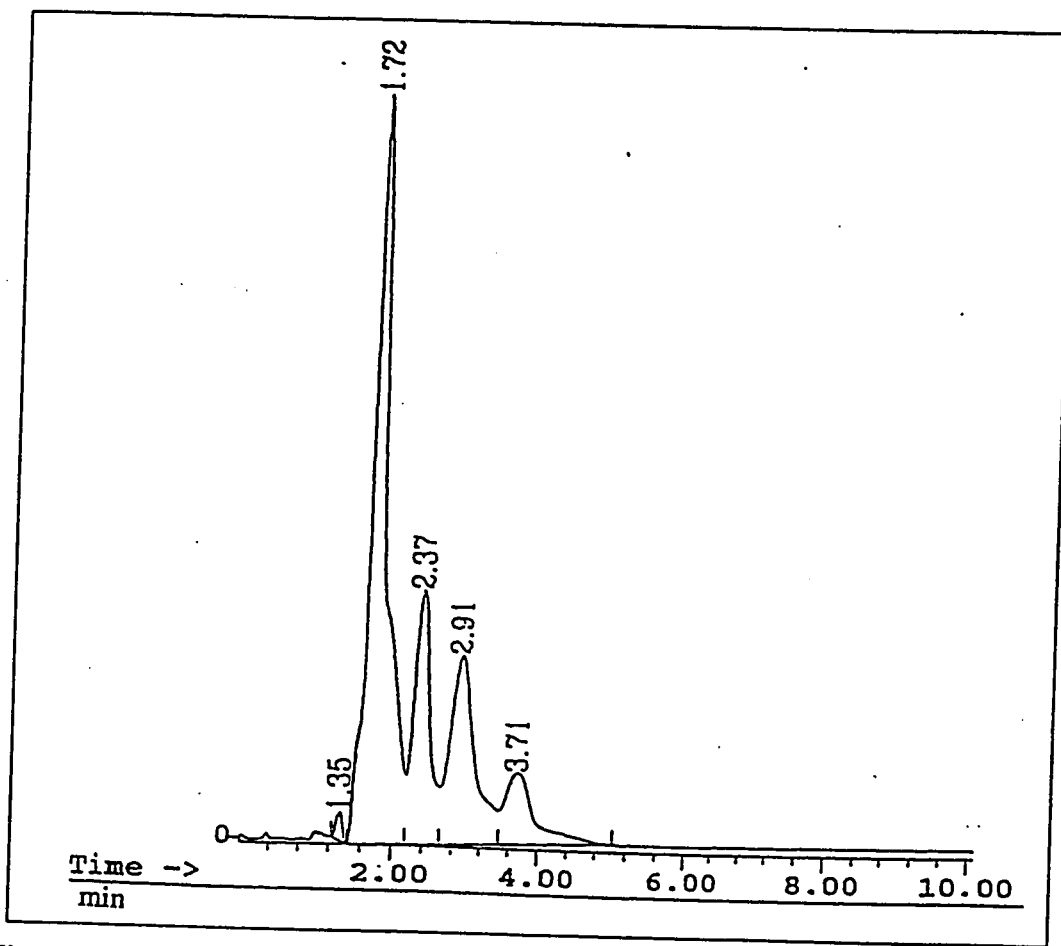


Figure 25. The Chromatogram of SRM 1647c on Column 1 with Gradient (i)

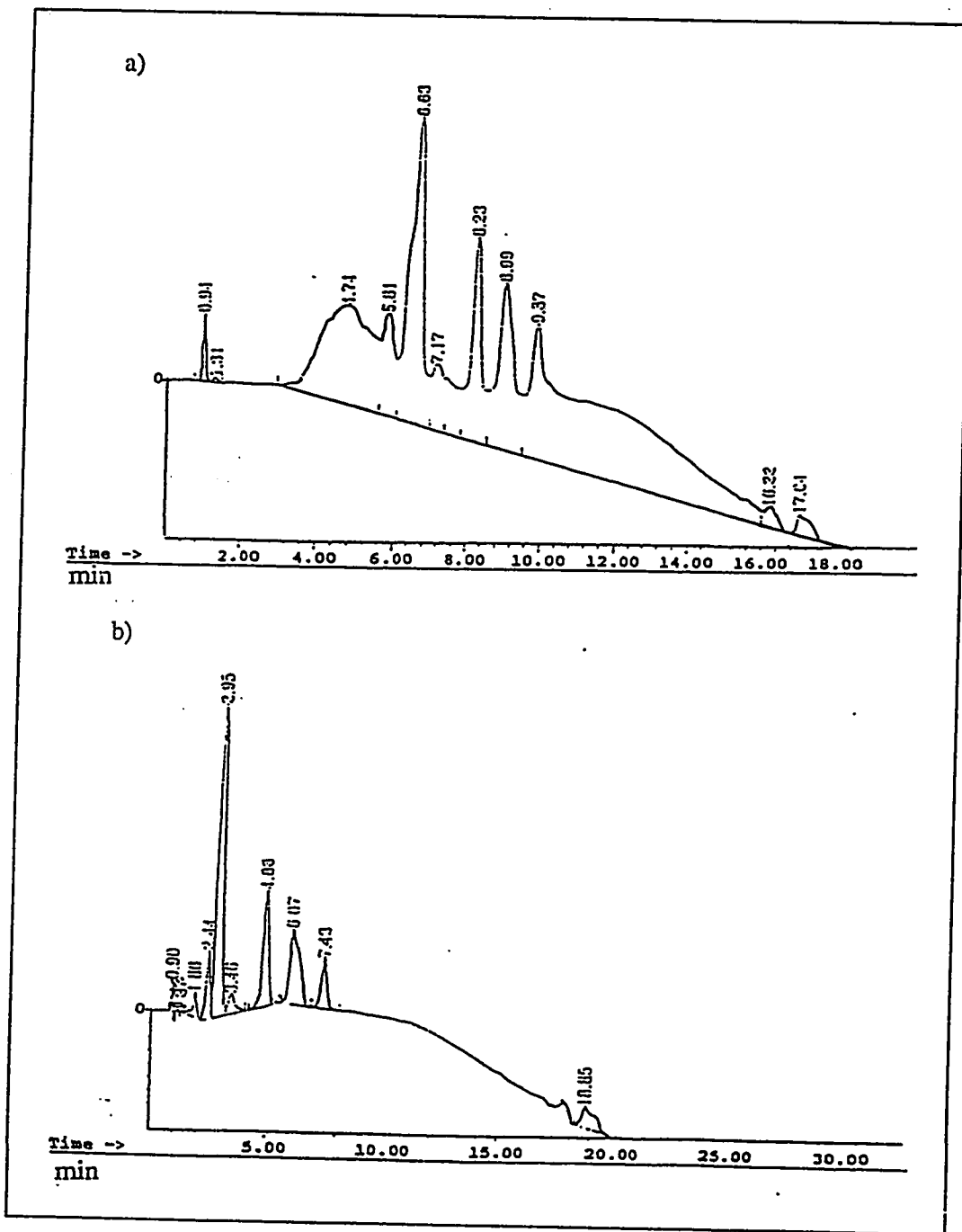


Figure 26. The Chromatograms of SRM 1647c on Column 2 with (a) Gradient (i) and (b) Gradient (ii)

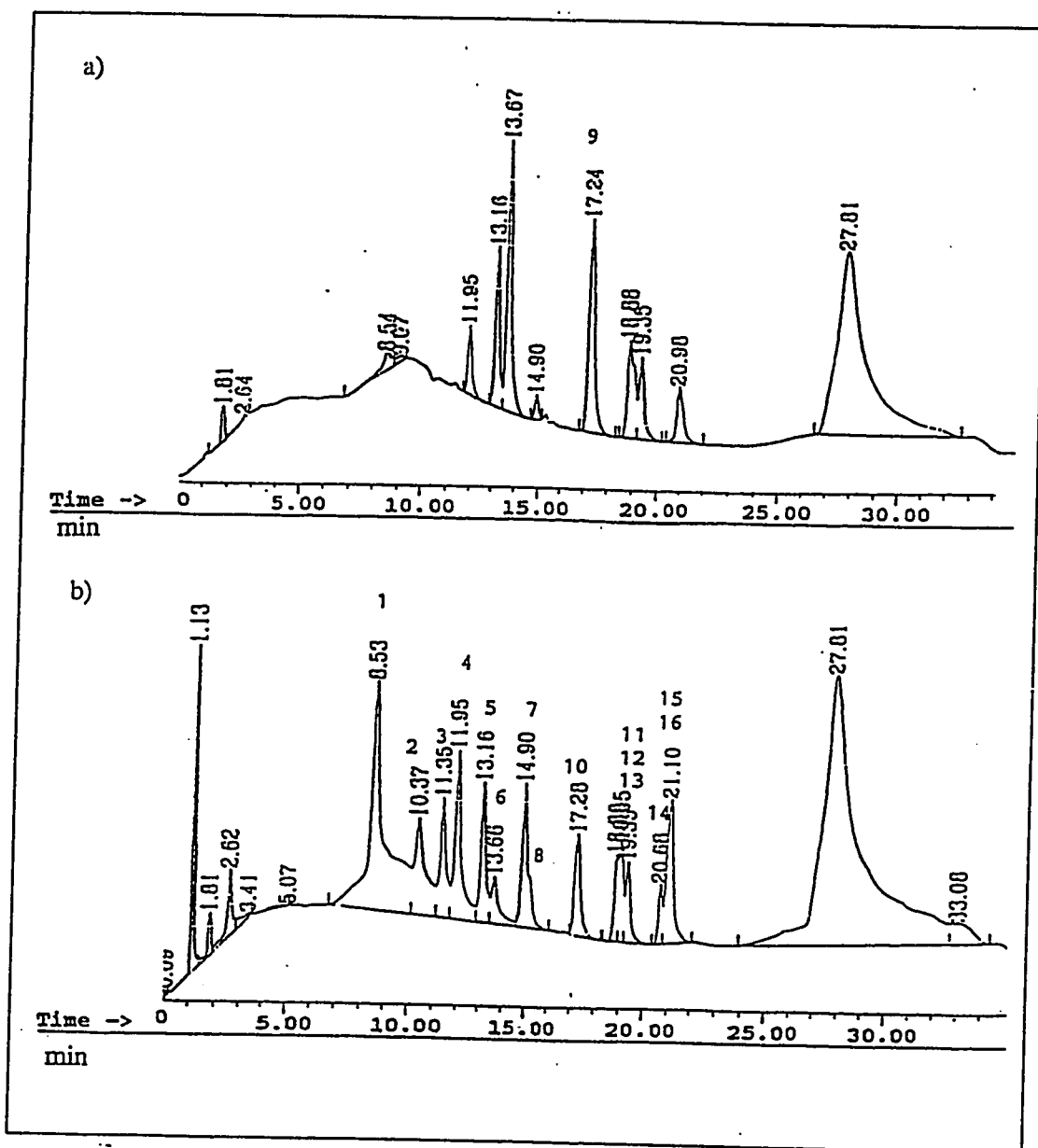


Figure 27. The Chromatograms of SRM 1647c on Column 3 with Gradient (iii) at (a) 254 and (b) 210 nm

(1) Naphthalene, (2) Acenaphthylene, (3) Acenaphthene, (4) Fluorene, (5) Phenanthrene, (6) Anthracene, (7) Fluoranthene, (8) Pyrene, (9) Benz[*a*]anthracene, (10) Chrysene, (11) Benzo[*b*]fluoranthene, (12) Benzo[*k*]fluoranthene, (13) Benzo[*a*]pyrene, (14) Dibenz[*a,h*]anthracene, (15) Benzo[*ghi*]perylene, (16) Indeno[1,2,3-*cd*]pyrene

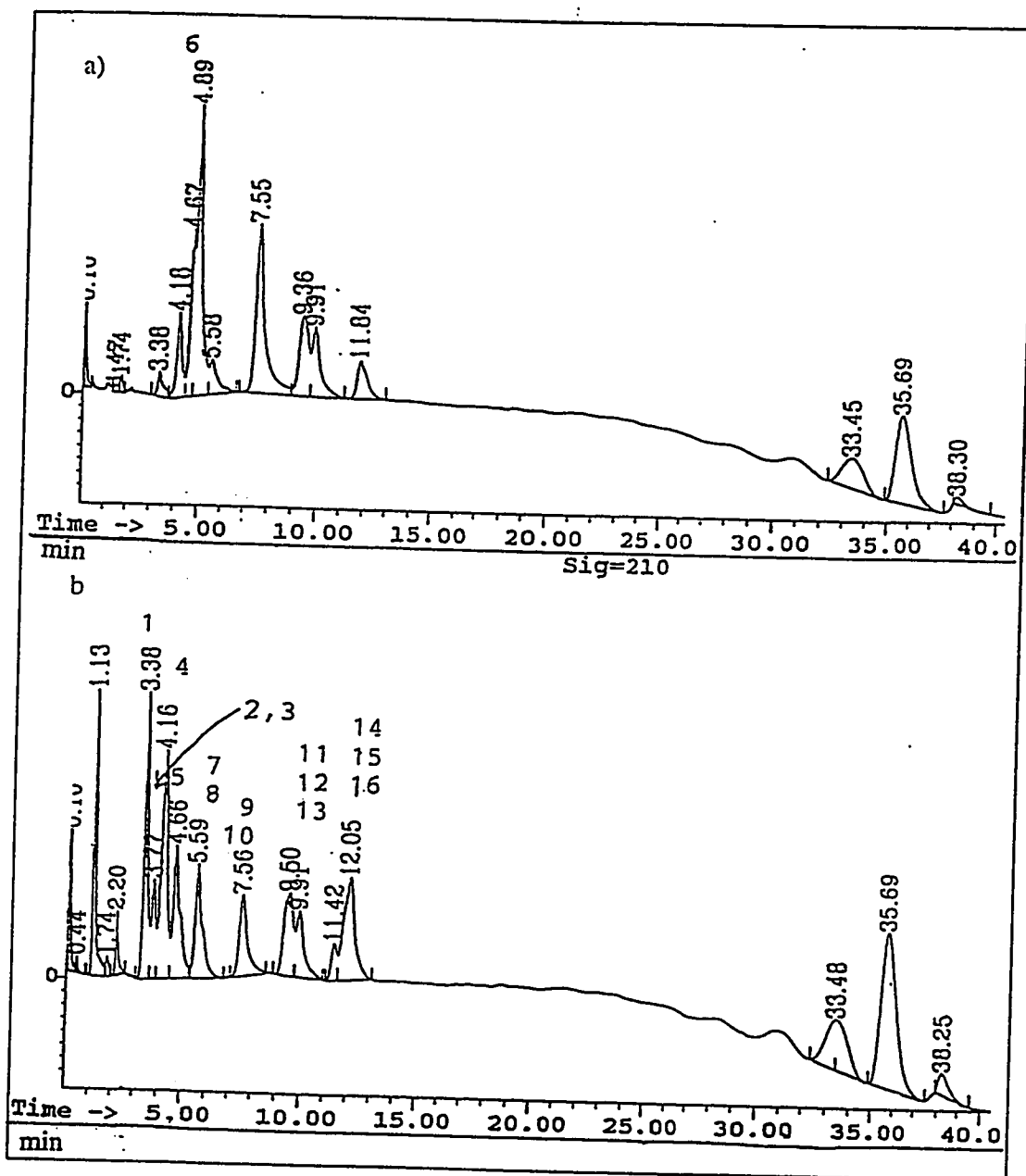


Figure 28. The Chromatograms of SRM 1647c on Column 3 with Gradient (iv) at (a) 254 and (b) 210 nm

(1) Naphthalene, (2) Acenaphthylene, (3) Acenaphthene, (4) Fluorene, (5) Phenanthrene, (6) Anthracene, (7) Fluoranthene, (8) Pyrene, (9) Benz[*a*]anthracene, (10) Chrysene, (11) Benzo[*b*]fluoranthene, (12) Benzo[*k*]fluoranthene, (13) Benzo[*a*]pyrene, (14) Dibenz[*a,h*]anthracene, (15) Benzo[*ghi*]perylene, (16) Indeno[1,2,3-*cd*]pyrene

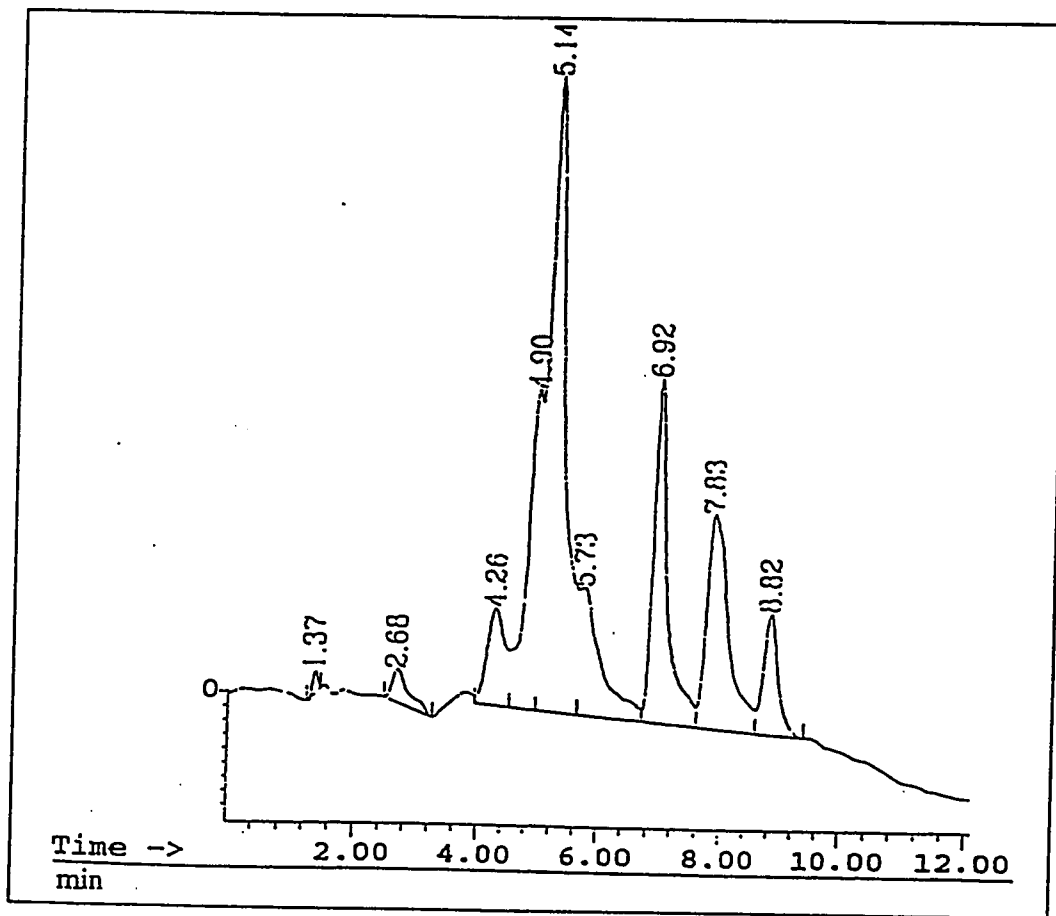


Figure 29. The Chromatogram of SRM 1647c on Column 1 with Gradient (vii)

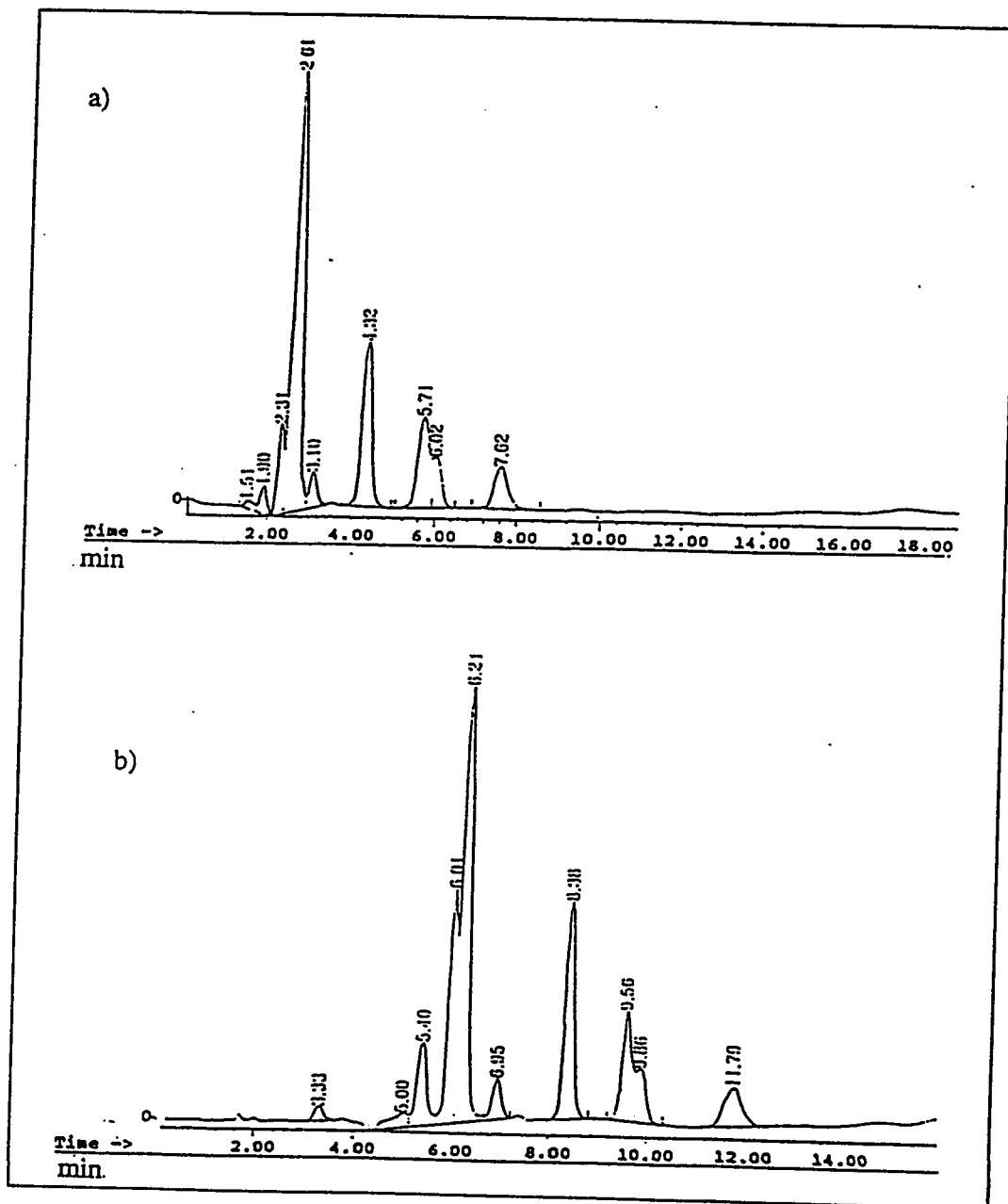


Figure 30. The Chromatograms of SRM 1647c on Column 2 with (a) Gradient (v) and (b) Gradient (vi)

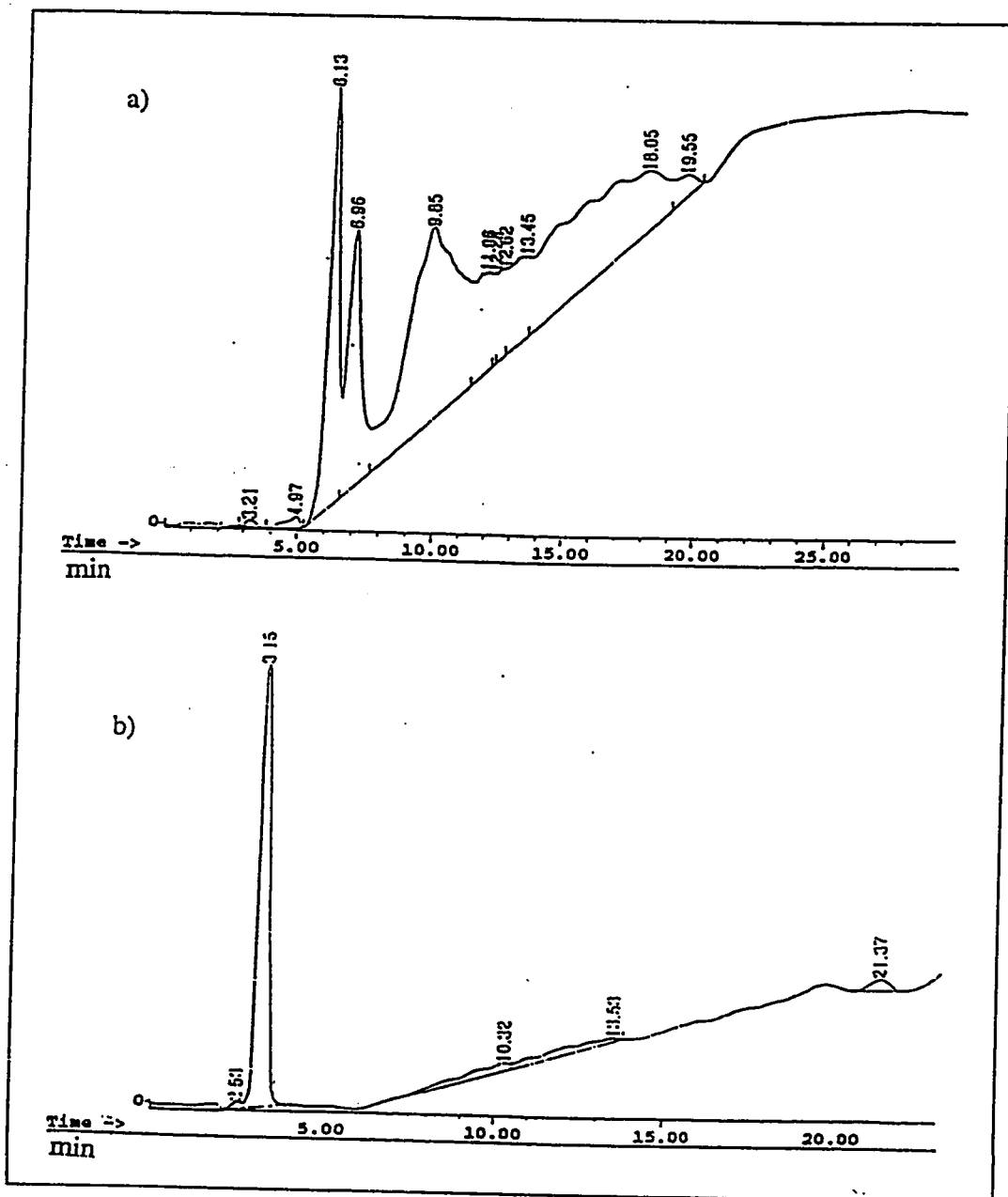


Figure 31. The Chromatograms of SRM 1647c on Column 2 with (a) Gradient (viii) and (b) Gradient (ix)

The chromatographic effect of the black zero-valent platinum is reflected on the chromatograms of columns 1, 2 and 3. The tailing observed for both columns 2 and 3 was not severe in comparison to column 1, which has a white stationary phase. Actually, zero-valent platinum usually complexes with ligands that possess empty π^* -antibonding orbitals, such as phosphine, cyanide, carbonyl and amine [20]. Therefore, the zero-valent platinum should not affect the PAH separations on the MPAB columns. The tailing on the MPAB columns may be caused by the sparse population of the organic moiety to shield the surface silanols.

3 . Column Characterization

Since column 3 has the best isomeric selectivity, its column efficiency was determined. Separation of a potassium nitrate-phenanthrene mixture was performed in triplicate with 60:40 ACN/water as the mobile phase and was detected at 254 and 210 nm. First, data was taken before column 3 was subject to any test sample (Figure 32a). The average number of theoretical plates, N , and average peak symmetry were 1957 and 0.73 respectively. The spreads were 440 for N and 0.03 for peak symmetry. After 32.8 hours of operation (Figure 32b), the average N and average peak symmetry increased to 4790 and 0.83 with a spread of 790 and 0.09 respectively. The differences in N before and after operations may be explained by the amount of mobile phase incorporated in between the bonded MPAB. During column packing, methanol drives the bonded silica into the

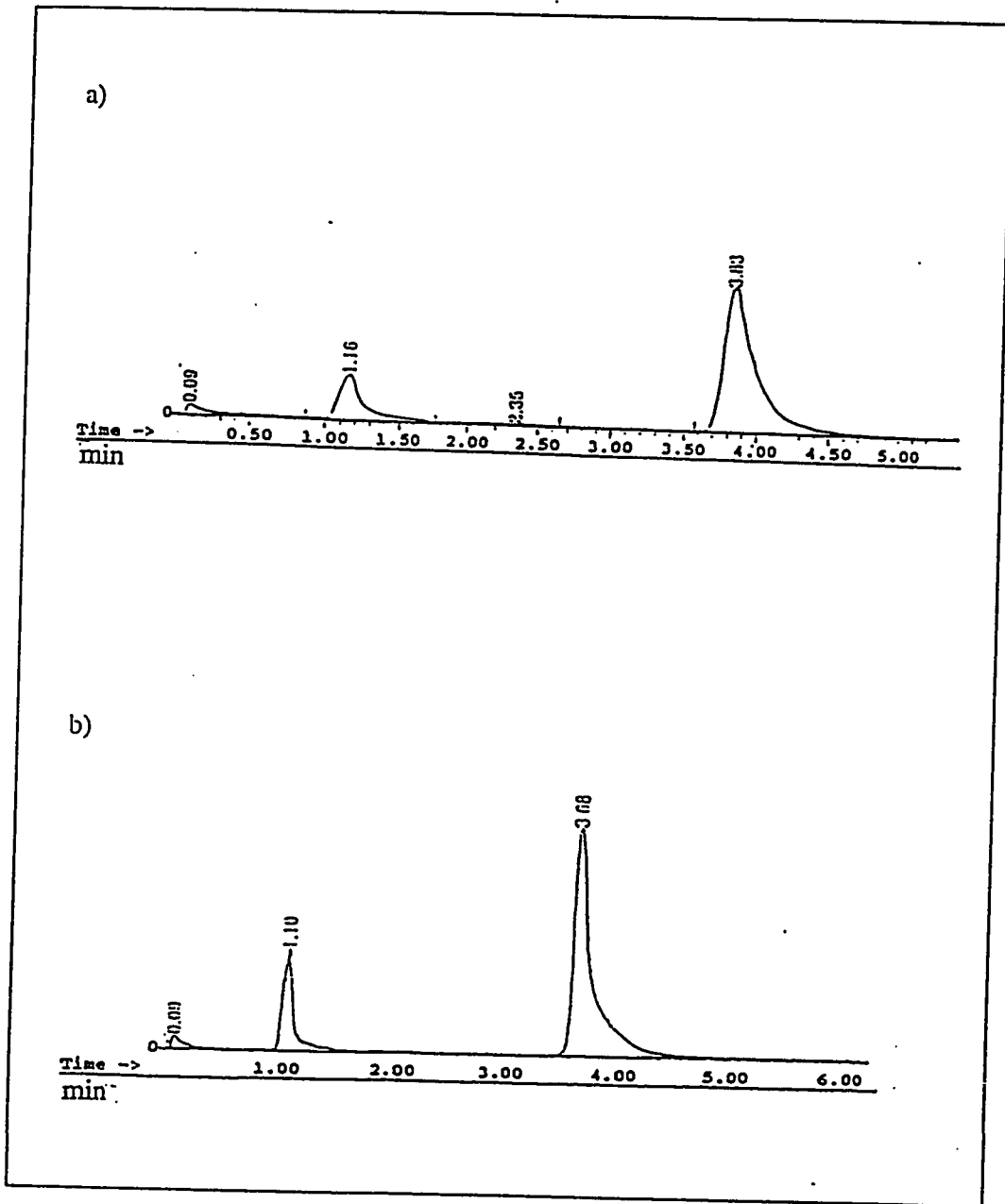


Figure 32. The Chromatograms of Column-Efficiency Determinations on Column 3 (a) Freshly Packed and (b) after 32.8 Hours of Operations (Flowrate of 1 ml/min.; mobile phase with 60:40 ACN/water; detection at 210 nm)

column. Naturally, methanol will be adsorbed between the bonded MPAB molecules. Even though column 3 was equilibrated with 60:40 ACN/water (a flat baseline was observed) before both efficiency tests, the proportion of methanol, acetonitrile and water trapped in the MPAB stationary phase may vary after 32.8-hours of diverse operating conditions. The configuration of the bonded MPAB molecules may change as well. Subsequently, the retention time of phenanthrene may be slightly altered. Consequently, N of phenanthrene before and after 32.8 hours of operation is also different under these circumstances.

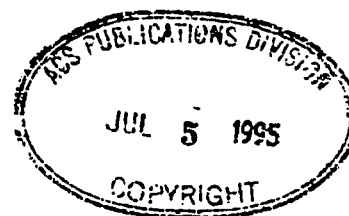
Chapter IV - Conclusion

Although its catalytic mechanism is not certain, hydrosilation catalyzed by chloroplatinic acid hexahydrate in isopentanol is successful. The best surface coverage achieved was $1.66 \mu\text{mol}/\text{m}^2$. The effects of surface coverage on chromatographic selectivity and separation behavior were studied. Increasing surface coverage causes MPAB ligands to interact more with their neighbors. An oligomeric-polymeric C18 like intermolecular arrangement is achieved at $1.66 \mu\text{mol}/\text{m}^2$. Resolution and isomeric selectivity are also enhanced at this surface coverage. The retention order of the several PAH solutes on the $1.66 \mu\text{mol}/\text{m}^2$ -MPAB phase may suggest that the retention mechanisms of the C18 and MPAB phases are comparable. Further work may focus on: (1) achieving higher surface coverages for the MPAB-bonded silica to improve isomeric separations, (2) investigating the catalytic mechanism of chloroplatinic acid hexahydrate in isopentanol, (3) optimizing the chromatographic conditions to resolve more structural isomers and (4) determining the retention mechanism of the MPAB stationary phase.

Chapter V - References

1. Speier, John L.; Webster, James A.; Barnes, Garrett H. *J. Am. Chem. Soc.* **1957**, *79*, 16-21.
2. Speier, John L. *Advances In Organometallic Chemistry* **1979**, *17*, 407-447.
3. Sandoval, J.E.; Pesek, J.J. *Anal. Chem.* **1991**, *63*, 2634-2641.
4. Skoog, D. A. *Principle Of Instrumental Analysis*, 3rd ed.; Saunders College Publishing: New York, 1985; p 784.
5. Dorsey, John G.; Cooper, William T. *Anal. Chem.* **1994**, *66*, 857A-867A.
6. Chu, C.; Jonsson, E.; Auvinen, M.; Pesek, J.J.; Sandoval, J.E. *Anal. Chem.* **1993**, *65*, 808.
7. Shah, S. M.S. Thesis, San Jose State University, May 1991.
8. Wise, S.A.; Sander, L.C. *J. High Resolution Chromatogr. and Chromatogr. Commun.* **1985**, *8*, 248-255.
9. Sander, L.C.; Wise, S.A. *CRC Crit. Rev. Anal. Chem.* **1987**, *18*, 299.
10. Pesek, J.; Cash, T. *Chromatographia* **1989**, *27*(11/12), 559-564.
11. Wheeler, John F.; Beck, Thomas L.; Klatte, S. J.; Cole, Lynn A.; Dorsey, John G. *J. Chromatogr. A* **1993**, *656*, 317-333.
12. Apfel, M.A.; Finkelmann, H.; Janini, G.M.; Laub, R.J.; Luhmann, B.H.; Price, A.; Roberts, W.L.; Shaw, T.L.; Smith, C.A. *Anal. Chem.* **1985**, *57*, 651-658.
13. Vogel, Israel *Vogel's Textbook of Practical Organic Chemistry, Including Qualitative Organic Analysis*, 4th ed.; Longman: New York, 1978; p 270.
14. Berendsen and De Galan *J. Liquid Chromatogr.* **1978**, *1*(5), 561-568
15. Dyer, John R. *Applications of Absorption Spectroscopy of Organic Compounds*; Prentice-Hall: Englewood Cliffs, NJ, 1965; p 25, pp 33-38.

16. Huang, Jianhua; Wu, Renjie *Gaofenzi Xuebao* 1992, 6, 742-747.
17. Chalk, A.J.; Harrod, J.F. *J. Am. Chem. Soc.* 1965, 87(1), 16-21.
18. Benkeser, Robert A.; Kang Jahyo *J. Organomet. Chem.* 1980, 185, C9-C12.
19. Chatt, J.; Duncanson, L. A. *J. Chem. Soc.* 1953, 2939.
20. Hartley, F.R. *The Chemistry of Platinum and Palladium*; John Wiley and Sons: New York, 1973; pp 12-13.
21. Ebbing, D. D. *General Chemistry*; Houghton Mifflin Company: Boston, 1984; pp 513-515.
22. Sander, Lane C; Wise, Stephen A. *J. Chromatogr.* 1984, 316, 163-181.
23. Jinno, K.; Kawasaki, K. *J. Chromatogr.* 1984, 316, 1-23.
24. Horvath, Csaba; Melander, Wayne *J. Chromatogr. Sci.* 1977, 15, 393-404.



Ruby Tam
3735 Goldfinch Terrace
Fremont, CA 94555

June 26, 1995.


ACS Copyright Office
Publications Division
1155 16th Street N.W.
Washington, DC 20036

Dear Sir:

I would like you to grant me a written reprint permission to use Figure 4 (page 508) of Sander, L.C.; Wise, S.A. Anal. Chem. 1984, 56, 504-510 in my master thesis (Tam, R. M.S. Thesis, San Jose State University, August 1995). This article has no copyright number. At the bottom of the first page of the article, "this article not subject to U.S. Copyright" is printed.

I would appreciate if you could reply by July 5, 1995. Should you have any question, please write or call me at 510-795-6810.

Sincerely,

| | |
|---|--|
|  PUBLICATIONS Division ACS 1155 - 15th St., N.W. Washington, DC 20036 | PERMISSION TO REPRINT IS GRANTED BY THE AMERICAN CHEMICAL SOCIETY |
| | ACS COPYRIGHT CREDIT LINE REQUIRED. Please follow this Sample: Reprinted with permission from [reference citation]. Copyright [year] American Chemical Society. |
| | APPROVED BY <u>G. Helen Courtney</u> ACS Copyright Office |
| 7-6-95 | |
| <input type="checkbox"/> If this box is checked, author permission is also required. See original article for address. | |

Ruby Tam
3735 Goldfinch Terrace
Fremont, CA 94555
June 26, 1995.

Marcel Dekker, Inc.
270 Madison Avenue
New York, NY 10016

Dear Sir:

I would like to obtain your written reprint permission to use Table 7 (pages 186-187) of Sander, L.C.; Wise, S.A. Advances in Chromatography 1986, 25, 139. in my master thesis (Tam, Ruby M.S. Thesis, San Jose State University, August 1995).

I would appreciate if you could reply by July 5, 1995. Should you have any question, please write or call me at (510) 795-6810.

Sincerely,



Debra Devere - Mount
6/27/95

PERMISSION GRANTED with the understanding that proper credit be given to Marcel Dekker Inc. Reference List should include:
Author's name (s). TITLE OF BOOK OR JOURNAL.
Volume____. Number____ Marcel Dekker, Inc., N.Y.
Year of Publication
Each item to be reprinted should carry the lines
Reprinted from Ref. (____). p. ____ by
courtesy of Marcel Dekker Inc.